CAPITAL UNIVERSITY OF SCIENCE AND
TECHNOLOGY, ISLAMABAD

Hybrid Nanofluid Flow between Parallel Plates

by

Qasim Mehmood

A thesis submitted in partial fulfillment for the
degree of Master of Philosophy

in the

Faculty of Computing
Department of Mathematics

2022

I am dedicating this heartfelt effort to my beloved family who supported me to conduct this research study and the respected teachers for helping and guiding to make a final output.

CERTIFICATE OF APPROVAL

Hybrid Nanofluid Flow between Parallel Plates

by

Qasim Mehmood

(MMT 183018)

THESIS EXAMINING COMMITTEE

S. No.	Examiner	Name	Organization
(a)	External Examiner	Dr. Tanvir Akbar	COMSATS, Islamabad
(b)	Internal Examiner	Dr. Rashid Ali	CUST, Islamabad
(c)	Supervisor	Dr. Dur-e-Shehwar Sagheer	CUST, Islamabad

Dr. Dur-e-Shehwar Sagheer
Thesis Supervisor
August, 2022

Dr. Muhammad Sagheer
Head
Dept. of Mathematics
August, 2022

Dr. Muhammad Abdul Qadir
Dean
Faculty of Computing
August, 2022

Author's Declaration

I, **Qasim Mehmood** hereby state that my MPhil thesis titled "**Hybrid Nanofluid Flow between Parallel Plates**" is my own work and has not been submitted previously by me for taking any degree from Capital University of Science and Technology, Islamabad or anywhere else in the country/abroad.

At any time if my statement is found to be incorrect even after my graduation, the University has the right to withdraw my MPhil Degree.

(Qasim Mehmood)
Registration No: MMT183018

Plagiarism Undertaking

I solemnly declare that research work presented in this thesis titled "**Hybrid Nanofluid Flow between Parallel Plates**" is solely my research work with no significant contribution from any other person. Small contribution/help wherever taken has been duly acknowledged and that complete thesis has been written by me.

I understand the zero tolerance policy of the HEC and Capital University of Science and Technology towards plagiarism. Therefore, I as an author of the above titled thesis declare that no portion of my thesis has been plagiarized and any material used as reference is properly referred/cited.

I undertake that if I am found guilty of any formal plagiarism in the above titled thesis even after award of MPhil Degree, the University reserves the right to withdraw/revoke my MPhil degree and that HEC and the University have the right to publish my name on the HEC/University website on which names of students are placed who submitted plagiarized work.

(Qasim Mehmood)
Registration No: MMT183018

Acknowledgement

Starting with the name of Almighty **ALLAH** who is most gracious and omnipresent, who makes the mankind and created this world to reveal what is veiled. Also, the **Prophet Muhammad (Peace Be Upon Him)** who is a guidance in every aspect of life for the betterment of Humanity. Firstly, I would like to express my deepest appreciation to my supervisor **Dr. Dur-e-shehwar Sagheer**, for the continual support of my MPhil research and also for her immense knowledge and enthusiasm. Without her tireless help, I would have not been able to commence this present research work. I could not have imagined having a better mentor and supervisor for my MPhil thesis. Besides my supervisor, I owe my profound gratitude to **Dr. Muhammad Sagheer** for his superb guidance and inexhaustible inspiration throughout this thesis. Without his tireless help, I would have not been able to commence this current research study. I am truly thankful to my teachers at Capital University of Science and Technology, **Dr. Rashid Ali, Dr. Abdul Rehman Kashif, Dr. Muhammad Afzal, Dr. Samina Rashid** and **Dr. Shafqat Hussain**. They are excellent teachers and I learnt a lot from them throughout the course of my M. Phil study. My most sincere and warm wishes to my friends especially university fellows **Bilal Javed, Sajid Ali, Mahzad Ahmed, Haseeb Chohan** and **Faisal Mehmood** who were always there as a source of encouragement for me. Further on, I am grateful to my colleagues of **GBES Khad**, my parents, wife and siblings for supporting me spirituality all over my life.

(Qasim Mehmood)

Abstract

The problem of hybrid nanofluid flow squeezed between two parallel plates while being affected by an magnetic inclination angle field is taken into consideration. The applied magnetic field inclination angle ranges from 0° degrees to 90° degrees. Additionally considered are viscous dissipation, Joule heating, and the lower plate stretching velocity with suction or injection. With the help of the shooting method and a fourth order Runge Kutta scheme, the transformed nonlinear governing equations are numerically solved. It is detailed how the velocity and temperature are affected by the squeeze number, the magnetic parameter, the magnetic inclination angle, the lower plate stretching parameter, the lower plate suction/injection parameter, and the Eckert number, respectively. It is discovered that the velocity and heat transfer in compressing flows are significantly influenced by the inclination angle of the applied magnetic field. By changing the magnetic field's angle of inclination, it is to roughly determine how a magnetic field strength affects velocity and temperature.

Contents

List of Figures

List of Tables

Abbreviations

BC	Boundary Condition
BVP	Boundary Value Problem
IVP	Initial Value Problem
MHD	Magnetohydrodynamics
ODEs	Ordinary Differential Equations
PDEs	Partial Differential Equations
RK	Runge Kutta

Symbols

(u, v)	Velocity components
(x, y)	Cartesian coordinates
u_s	velocity of lower plate
v_H	velocity of upper plate
v_c	lower plate mass flux velocity
Cp	Specific heat constant $(Jkg^{-1}K^{-1})$
ρ	Fluid density
κ	Thermal conductivity
μ	Viscosity
ρ	Density
ν	Kinematic viscosity
α	Thermal diffisuitivity
σ	Electrical conductivity
B_0	Magnetic field constant
T	Temperature
T_0	Temperature of lower plate surface
T_H	Temperature of upper plate surface
ρ_f	Density of the base
μ_f	Viscosity of the base fluid
ν_f	Kinematic viscosity of the base fluid
κ_f	Thermal conductivity of the base fluid
Cp_f	Specific heat constant of the base fluid
$(\rho Cp)_f$	Heat capacitance of the base fluid

ρ_{hnf}	Density of the hybrid nanofluid
μ_{hnf}	Viscosity of the hybrid nanofluid
ν_{hnf}	Kinematic viscosity of the base hybrid nanofluid
κ_{hnf}	Thermal conductivity of the hybrid nanofluid
Cp_{hnf}	Specific heat constant of the hybrid nanofluid
$(\rho Cp)_{hnf}$	Heat capacitance of the base hybrid nanofluid
C_f	Skin friction coefficient
Nu	Nusselt number
Re	Reynolds number
Re_x	Local Reynolds number
ϕ	Nanoparticle volume fraction
M	Magnetic parameter
Ec	Eckert number
Pr	Prandtl number
S	Squeeze number
R	Lower plate stretching parameter
S_b	Lower plate suction/injection parameter
γ	Magnetic inclination angle
f	Dimensionless velocity
θ	Dimensionless temperature

Chapter 1

Introduction

When two plates move closer to each other, viscous fluids between the plates exhibit a squeezing motion, which is normal to the plate surfaces. There are various industrial uses for the squeezing flow, including liquid-metal lubricated bearings, food processing, injection moulding, compression, squeezed films in power transmission, cooling water, etc. Researchers are very interested in the analysis of velocity and heat transfer in the squeezing flow between parallel plates because of its broad range of practical applications. The first study about the squeezing flow was reported by Stefan [1], when he investigated the lubrication system. Stefan's pioneering research opened up new paths and beneficial perspectives for the study of squeezing flow. Later on, several expanding investigations on the squeezing flow have been done. Squeezing flow investigation has received much attention in recent years from a variety of research angles. In 2009, Ran et al. [2] explored a quasi-steady axisymmetric Newtonian fluid squeezed between two parallel plates and used the homotopy analysis method to get an explicit series solution of the dimensionless velocity. In 2009, heat and mass transfered in the unsteady squeezing flow between parallel plates examined by Mustafa et al. [3]. Khan et al. [4] obtained approximate analytical solutions for the squeezing flow of nanofluid under the influence of viscous dissipation and velocity slip. Domairry et al. [5] used a Duan-Rach method to discover an approximate analytical solution of the unsteady squeezing flow of a nanofluid. Hayat et al. [6] investigated the influence

of convective circumstances and chemical reactions on squeezing flow. In 2021, Ahmad et al. [7] analyzed the impact of velocity, thermal and solutal slips effects on squeezed fluid transport features. Hayat and Hina [6] discussed the effect on Williamson fluid flow through mass and heat transfer with exible walls. Ahmad et al. [8] aimed to theoretically examine the mixed convection characteristics in the squeezing flow of Sutterby fluid in squeezed channel.

To maintain flow and heat transfer under the application of magnetic field has important significance for multiple areas of physics, especially nuclear reactors with MHD generators, geothermal extractions, plasma studies, aeronautical and aerodynamic boundary layer control, etc. [9–22]. Recently, researchers have attempted to investigate many elements and methodologies of the transfer behaviors of conducting fluid between squeezing surfaces under the influence of magnetic fields. The influence of a magnetic field on the unsteady hydromagnetic squeezing flow of an incompressible two-dimensional viscous fluid between two infinite parallel plates studied by Siddiqui et al. [23]. In the presence of a magnetic field, the squeezing flow between parallel disks were examined by Domairry et al. [5]. In 2015, Haq et al. [24] investigated the squeezed movement of nanofluid over a sensor surface using MHD. Under the influence of magnetic fields the flow of nanofluid squeezed over a porous stretched surface explored by Hayat et al. [6]. A slip analysis on the fluid-solid interface in the MHD squeezing flow of Casson fluid through Porous Medium was presented by Khan et al. [25].

The magnetic fields which are being used in the squeezing flow discussed above are perpendicular to the solid surface. On the other hand, we must take into consideration that inclined magnetic fields might cause fluid flow issues that are significantly more challenging and widely existent. In 2011, Hayat et al. [6] focused on the impacts of inclined magnetic fields in their investigations of the flow and heat transfer properties of Williamson fluid in a channel and nanofluid in an open cavity, respectively. Rashad et al. [26] investigated the free convection flow in a rectangular cavity in the presence of a uniform angled magnetic field. The research on the squeezing flow subjected to angled magnetic fields needs further investigation, according to the survey of related literatures that we have found.

Acharya et al. [27] investigated the squeezing movement of Cu-water and Cu-kerosene nanofluids flow between two parallel plates. Devi et al. [28] investigated numerically the hydromagnetic hybrid $Cu - Al_2O_3$/water nanofluid flow over a permeable stretching sheet with suction. In 2020, Waini et al. [29] examined the squeezing hybrid nanofluid flow over a permeable sensor surface with magneto-hydrodynamics (MHD) and radiation effects. The Alumina (Al_2O_3) and Copper (Cu) are considered as the hybrid nanoparticles and water is the base fluid.
Inspired by the above studies, the present investigation intends to explore the flow and heat transfer characteristics of squeezed hybrid nanofluid flow between two parallel plates under the influence of magnetic inclination angle field. In this squeezing flow, the surface of the lower plate with suction/injection is stretching along the longitudinal direction. In addition, the effects of viscous dissipation and Joule heating are also taken into account. By solving the resulting governing equations numerically, the effects of the squeeze number, the magnetic parameter, the magnetic inclination angle, the lower plate stretching parameter, the lower plate suction/injection parameter and Eckert number on the longitudinal velocity and temperature are examined.

1.1 Thesis Contribution

In this thesis, a review study of Su and Yin [30] has been presented and then the flow analysis has been extended in hybrid nanofluid flow. The Alumina (Al_2O_3) and Copper (Cu) are considered as the hybrid nanoparticles and water is the base fluid. The governing system of nonlinear PDEs is converted into a model of nonlinear ODEs by using appropriate transformation of similarities. Numerical results are obtained for the set of nonlinear ODEs by using the shooting technique with Runge Kutta method of order four (RK4). The influence of various relevant physical parameters has been discussed using graphs.

1.2 Thesis Framework

This research work is further classified into four main chapters.

Chapter 2 contains some basic definitions, terminologies and governing equations of the fluid which are needed for the upcoming chapters.

Chapter 3 contains the review work of Su and Yin [30], the effects of an inclined magnetic field on the unsteady squeezing flow between parallel plates with suction or injection. By utilizing similarity transformation we reduce the set of nonlinear PDEs into a set of nonlinear ODEs and then solve numerically. Numerical results are obtained for the set of nonlinear ODEs with the help of shooting technique.

Chapter 4 extends the work of Su and Yin [30] by considering hybrid nanofluid flow between parallel plates. The transformation of similarities has been utilized for the conversion of PDEs to ODEs. The transformed nonlinear ODEs are then solved by using the shooting technique that is most common.

Chapter 5 summarizes the research work and gives the main conclusion arising from the whole study.

All the references used in this thesis are presented in Bibliography.

Chapter 2

Basic Terminologies and Governinig Equations

In this chapter, some basic laws, concepts, terminologies and definitions are defined. These concepts are necessary for the work presented in the incoming chapters.

2.1 Fluid and its Properties

Scientists across the several fields study fluid dynamics. To study the problems in fluid dynamics it is indispensable to explain properties of fluids.

Definition 2.1.1 (Fluid)
"A fluid is defined as a substance that deforms continuously when acted on by a shearing stress of any magnitude. A shearing stress (force per unit area) is created whenever a tangential force acts on a surface."[31]

Definition 2.1.2 (Fluid Mechanics)
"Fluid mechanics is defined as science that deals with the behavior of fluids at rest (fluid statics) or in motion (fluid dynamics), and the interaction of fluids with

solid or other fluids at the boundaries."[32]

Definition 2.1.3 (Fluid Dynamics)

"The branch of fluid mechanics that covers the properties of the fluid in the state of progression from one place to another is called fluid dynamics." [33]

Definition 2.1.4 (Fluid Statics)

"It is the field of physics that involves the study of fluids at rest. These fluids are not in motion, that means they have achieved a stable equilibrium state, so fluid statics is largely about understanding these fluid equilibrium conditions." [33]

Definition 2.1.5 (Pressure)

"The continuous physical force exerted on the unit area of surface is said to be pressure. It is expressed by P and mathematically, it can be written as,

$$P = \frac{F}{A},$$

where F and A denote the applied physical force and area of the surface."[34]

Definition 2.1.6 (Density)

"Density is defined as the mass per unit volume. that is,

$$\rho = \frac{m}{V},$$

where m and V are the mass and volume of the substance, respectively."[32]

Definition 2.1.7 (Viscosity)

"Viscosity of a fluid is defined as the measure of resistance to steady distortion by shear/tensile stress. A notation used for viscosity is μ and its mathematical expression is,

$$\mu = \frac{\text{shear stress}}{\text{rate of shear strain}},$$

where μ is called the coefficient of absolute viscosity/dynamics viscosity or simple viscosity. The dimension of viscosity is $\left[\frac{M}{LT}\right]$." [34]
Water is a thin fluid having low viscosity and on other hand honey is thick fluid carrying higher viscosity. Usually liquids have non-zero viscosity.

Definition 2.1.8 (Kinematics Viscosity)
"The ratio of dynamic viscosity to density appears frequently. For convenience, this ratio is given the name kinematic viscosity ν and is expressed as,

$$\nu = \frac{\mu}{\rho},$$

where μ denotes dynamic viscosity and ρ denotes density respectively." [32]

Definition 2.1.9 (Nanofluid)
"The nanofluid is defined as the homogeneous mixture of the base fluid and nanoparticles. The nanoparticles used in nanofluids are typically made of metals, oxides, copper, carbides or carbon nanotubes." [34]

2.2 Classification of Fluid

The following are some important types of fluid.

Definition 2.2.1 (Ideal Fluid)
"A fluid which is incompressible and has no viscosity is known as an ideal fluid." [35]

Definition 2.2.2 (Real Fluid)
"A fluid which possesses viscosity is known as a real fluid. All the fluids in actual practice are real fluids." [35]

Definition 2.2.3 (Newtonian Fluid)

"A real fluid in which shear stress is directly proportional to the rate of shear strain (or velocity gradient) is known as a Newtonian fluid."[35]
The common examples of Newtonian fluids are air, oxygen gas, alcohol, milk, glycerol and silicone/thin motor oil etc.

Definition 2.2.4 (Non-Newtonian Fluid)
"A real fluid in which the shear stress is not proportional to the rate of shear strain (or velocity gradient) is known as a Non-Newtonian fluid."[35]
Examples of Non-Newtonian fluids are toothpaste, ketchup, starch suspensions, custard, maizena, shampoo, paint and blood etc.

2.3 Types of Fluid Flow

In this section, we discuss some basic types of fluid flow with their examples.

Definition 2.3.1 (Flow)
"It is the deformation of the material under the influence of different forces. If the deformation increase is continuous without any limit then the process is known as flow."[33]

Definition 2.3.2 (Laminar and Turbulent Flow)
"When the fluid partical follows a smooth trajectory, the flow is then said to be laminar. Further increases in speed may lead to instability that eventually produces a more random type of flow that is called turbulent."[36]
Examples of laminar flow are blood flow, aircrafts, rivers/canals etc.
Examples of turbulent flow are blood flow in arteries, oil transport in pipelines, lava flow etc.

Definition 2.3.3 (Steady and Unsteady Flow)
"A flow is said to be steady flow in which the fluid properties do not change with time at a specific point. Mathematically, it can be written as,

$$\frac{\partial \lambda}{\partial t} = 0,$$

where λ is any fluid property. A flow is said to be unsteady flow in which fluid properties change with time. Mathematically, it can be written as,

$$\frac{\partial \lambda}{\partial t} \neq 0.\text{"}[33]$$

Examples of steady flow are pipes, nozzles, diffusers, pumps etc.
Examples of unsteady flow are passage of a flood wave, operation of irrigation and power canals, tidal effects, junctions, measures to control floods etc.

Definition 2.3.4 (Compressible Flow)

"A flow in which the density variation is not negligible is known as compressible flow."[37]
Examples include aerodynamic applications such as flow over a wing or aircraft nacelle as well as industrial applications such as flow through high-performance valves.

Definition 2.3.5 (Incompressible Flow)

"A flow in which the density remains constant throughout is known as incompressible." [37]
Example of incompressible fluid flow is, the stream of water flowing at high speed from a garden hose pipe.

Definition 2.3.6 (Rotational Flow)

"Rotational flow is that type of flow in which the fluid particles while flowing along stream-lines, also rotate about their own axis."[35]
An example is the flow of water in a pipe of constant diameter at constant velocity.

Definition 2.3.7 (Irrotational Flow)

"Irrotational flow is that type of flow in which the fluid particles while flowing

along stream-lines, do not rotate about their own axis then this type of flow is called irrotational flow."[35]

Definition 2.3.8 (External Flow)

"The flow which is not bounded by the solid surface, is known as external flow." [38]

The flow of water in the ocean or in the river is an example of the external flow.

Definition 2.3.9 (Internal Flow)

"Fluid flow which is bounded by the solid surface is called internal flow." [38]

The examples of the internal flow are the flow through pipes or glass.

2.4 Heat Transfer Mechanism and Related Properties

Heat transfer is a phenomena that convey energy and entropy from one location to another. The formal definition of heat transfer is provided as follows:

Definition 2.4.1 (Heat Transfer)

"Heat transfer is a branch of engineering that deals with the transfer of thermal energy from one point to another within a medium or from one medium to another due to the occurrence of a temperature difference." [39]

Following are the important modes of heat transfer.

Definition 2.4.2 (Conduction)

"Conduction is the process in which heat is transferred through the material between the objects that are in physical contact."[33]

Examples of conduction are, a lizard warming its belly on a hot rock, touching a hot seatbelt when you get into a car.

Definition 2.4.2 (Convection)

"Convection is a mechanism in which heat is transferred through fluids (gasses or liquids) from a hot place to a cool place."[33]

Examples of convection are, boiling water, air conditioner, body blood circulation, melting of chilled drinks, refrigerator etc.

Convection is subdivided into the following three types.

Definition 2.4.3 (Forced Convection)

"Forced convection is a process in which fluid motion is produced by an external source. It is a special type of heat transfer in which fluid moves in order to increase the heat transfer. In other words, a method of heat transfer in which heat transfer is caused by dependent source like a fan and pump etc, is called forced convection."[40]

Examples of forced convection are using water heaters or geysers for instant heating of water and using a fan on a hot summer day.

Definition 2.4.4 (Natural Convection)

"Natural convection is a heat transport process, in which the heat transfer is not caused by an external source, like pump, fan and suction. It happens due to the temperature differences which affect the density of the fluid. It is also called free convection. "[40]

The most common examples of the natural convection are:

Sea breeze: This phenomenon occurs during the day. The sun heats up both the sea surface and land.

Land Breeze: This phenomenon occurs during the night when the situation reverses.

Definition 2.4.5 (Mixed Convection)

"A method in which both forced and natural convection processes simultaneously and significantly involve in the heat transfer is called mixed convection."[40]

An example of this is a fan blowing upward on a hot plate.

Definition 2.4.6 (Thermal Radiation)

"The ejection of electromagnetic waves from the matters that have temperature higher than absolute zero is called thermal radiation."[34]

For example: Daily weather.

Definition 2.4.7 (Thermal Conductivity)

"Thermal conductivity (κ) is the property of a material related to its ability to transfer heat. Mathematically,

$$\frac{dQ}{dt} = -\kappa A \left(\frac{dT}{dx}\right),$$

where A, k, $\frac{dQ}{dt}$, $\frac{dT}{dx}$ are the area, thermal conductivity, the rate of heat transfer and the temperature gradient respectively. With the increase of temperature, thermal conductivity of most liquids decreases except water. The SI unit of thermal conductivity is $\frac{Kg.m}{s^3}$ and its dimension is $\frac{ML}{T^3}$." [40]

Definition 2.4.8 (Thermal Diffusivity)

" The ratio of the unsteady heat conduction κ of a substance to the product of specific heat capacity C_p and density ρ is called thermal diffusivity.

$$\alpha = \frac{k}{\rho C_p}.$$

The unit and dimension of thermal diffusivity in SI system are $\frac{m^2}{s}$ and $[LT^{-1}]$ respectively."[37]

2.5 Dimensionless Numbers

The following dimensionless number will appear in the discussion given in next chapters.

Definition 2.5.1 (Skin Friction)

" Skin friction coefficient represents the value of friction which occurs when fluid moves across the surface. Mathematically,

$$C_f = \frac{2\tau_\omega}{\rho U_e^2},$$

where τ_ω is the shear stress at the wall, ρ the density and U_e the free-stream velocity." [41]

Definition 2.5.2 (Nusselt Number)

" The hot surface is cooled by a cold fluid stream. The heat from the hot surface, which is maintained at a constant temperature, is diffused through a boundary layer and convected away by the cold stream. Mathematically,

$$Nu = \frac{qL}{\kappa},$$

where q stands for convective heat transfer, L for the characteristics length and κ stands for the thermal conductivity."[42]

Definition 2.5.3 (Prandtl Number)

"The ratio between the momentum diffusivity ν and thermal diffusivity α is called Prandtl number. Mathematically, it can be defined as,

$$Pr = \frac{\nu}{\alpha} = \frac{\mu C_p}{\kappa},$$

where μ represents the dynamic viscosity, C_p denotes the specific heat and κ stands for thermal conductivity. The relative thickness of thermal and momentum boundary layer is controlled by Prandtl number."[40]

Definition 2.5.4 (Reynolds Number)

" It is a dimensionless number which is used to clarify the different flow behaviours like turbulent or laminar flow. It helps to measure the ratio between inertial force and the viscous force. Mathematically,

$$Re = \frac{LU}{\nu},$$

where U denotes the free stream velocity, L the characteristics length. At low Reynolds number, laminar flow arises where the viscous forces are dominant. At high Reynolds number, turbulent flow arises where the inertial forces are dominant."[40]

Definition 2.5.5 (Eckert Number)

" It is the proportion of the kinetic energy dissipated in the flow to the thermal energy conducted into or away from the fluid."[41]

2.6 Conservation Laws

Several conservation laws such as the law of conservation of mass, energy and momentum are of great importance for the researchers. These laws are applied to closed systems and then extended to region in space called controlled volumes. We now give a brief discussion of some important conservation laws.

Definition 2.6.1 (Conservation of mass)

" The principle of conservation of mass can be stated as the time rate of change of mass is fixed volume is equal to the net rate of flow of mass across the surface. Mathematically, it can be written as:

$$\frac{\partial \rho}{\partial t} + \nabla.(\rho \mathbf{u}) = 0,$$

where t is time, the fluid density is ρ, and the fluid velocity is $\mathbf{u}$." [39]

Definition 2.6.2 (Conservation of Momentum)

" The momentum equation states that the time rate of change of linear momentum of a given set of particles is equal to the vector sum of all the external forces acting on the particles of the set, provided Newton's third law of action and reaction governs the internal forces. Mathematically, it can be written as:

$$\frac{\partial}{\partial t}(\rho \mathbf{u}) + \nabla.[(\rho \mathbf{u})\mathbf{u}] = \nabla.\mathbf{T} + \rho g."[39]$$

Definition 2.6.3 (Conservation of Energy)

"The law of conservation of energy states that the time rate of change of the total energy is equal to the sum of the rate of work done by the applied forces and change of heat content per unit time.

$$\frac{\partial \rho}{\partial t} + \nabla.\rho \mathbf{u} = -\nabla.\mathbf{q} + Q + \phi,$$

where ϕ is a dissipation function, q is heat generation parameter and Q is heat constant." [39]

2.7 Solution Methodology

Shooting method is used to solve the higher order non-linear ordinary differential equations. To implement this technique, we first convert the higher order ODEs to the system of first order ODEs. After that we assume the missing initial conditions and the differential equations are then integrated numerically using the Runge Kutta method as an initial value problem. The accuracy of the assumed missing initial condition is then checked by comparing the calculated values of the dependent variables at the terminal point with their given value there. If the boundary conditions are not fulfilled up to the required accuracy, with the new set of initial conditions, then they are modified by Newtons method. The process

is repeated again until the required accuracy is achieved. To explain the shooting method, we consider the following general second order boundary value problem.

$$g''(x) = f(x, g, g'(x)) \tag{2.1}$$

along with the boundary conditions:

$$g(0) = 0, \qquad g(Q) = Z. \tag{2.2}$$

To have a system of first order ODEs, used the notations:

$$g = g_1, \qquad g_1' = g_2. \tag{2.3}$$

By using the notations (2.3) in (2.1) and (2.2), we have the following IVP:

$$\left.\begin{aligned} g_1' &= g_2, & g_1(0) &= 0, \\ g_2' &= f(x, g_1, g_2), & g_2(0) &= h. \end{aligned}\right\} \tag{2.4}$$

Now, the initial value problem satisfy the boundary condition $g_1(Q) = Z$,

$$g_1(Q, h) - Z = \phi(h) = 0. \tag{2.5}$$

To find an approximate root of (2.5) by the Newton's method, is written as,

$$h_{n+1} = h_n - \frac{\phi(h_n)}{(\frac{\partial \phi}{\partial h})_{h=h_n}}, \tag{2.6}$$

or

$$h_{n+1} = h_n - \frac{g_1(h_n) - Z}{\frac{\partial}{\partial h}\left[g_1(h) - Z\right]_{h=h_n}}. \tag{2.7}$$

To implement the Newton's method, consider the following notations,

$$\frac{\partial g_1}{\partial h} = g_3, \qquad \frac{\partial g_2}{\partial h} = g_4. \tag{2.8}$$

These new notations will give the Newton's iterative scheme its form,

$$h_{n+1} = h_n - \frac{g_1(h) - Z}{g_3(h)}. \tag{2.9}$$

Now, differentiating (2.4) w.r. to h, we get:

$$\left.\begin{aligned} g_3' &= g_4, & g_3(0) &= 0. \\ g_4' &= g_3\frac{\partial f}{\partial g_1} + g_4\frac{\partial f}{\partial g_2}, & g_4(0) &= 1. \end{aligned}\right\} \tag{2.10}$$

Rewriting the above four first order ODE's (2.4) and (2.10) together, we have the following IVP:

$$\begin{aligned} g_1' &= g_2, & g_1(0) &= 0. \\ g_2' &= f(x, g_1, g_2), & g_2(0) &= h. \\ g_3' &= g_4, & g_3(0) &= 0. \\ g_4' &= g_3\frac{\partial f}{\partial g_1} + g_4\frac{\partial f}{\partial g_2}, & g_4(0) &= 1. \end{aligned}$$

Runge Kutta method of order four will be used to numerically solve the above system as a whole.
the Newton's technique stopping criteria is set as:

$$|g_1(h) - Z| < \epsilon,$$

for an arbitrarily small positive value of ϵ.

Chapter 3

Effect of Inclined Magnetic Field for Squeezing Flow

3.1 Introduction

In this chapter the detailed analysis of the work presented by Su and Yin [30] is discussed. The description of the empirical research of inclined magnetic field effects with suction/injection between parallel plates on the unsteady squeezing flow is reviewed in this study. By using suitable similarity transformations, the controlling partial differential equations are converted into ordinary differential equations. The numerical solution for the differential equations are obtained by utilizing the shooting technique. Graphs are represented to show the physical significance of distinct dimensionless quantities. By varying the values of the different parameters, we observed the trend of the velocity and temperature distributions.

3.2 Mathematical Modeling

Considering the unsteady squeezing flow of an incompressible fluid electrically conducted fluid which is confined between two infinite parallel plates. The flow is subjected to an inclined external magnetic field **B**. The lower plate channel

is along the x-axis, so it is normal to the y-axis. Consider the time dependent magnetic field

$$\mathbf{B} = (B_m \cos\gamma, B_m \sin\gamma, 0)\,,$$

in which B_m denotes $B_0(1-\alpha t)^{\frac{-1}{2}}$ and γ is the angle of inclination with respect to x-axis. The induced magnetic field is assumed to be negligible for a small magnetic Reynolds number. The gap between two plates

$$H(t) = l(1-\alpha t)^{\frac{1}{2}},$$

changes with the time t, where l is the initial gap between the plates at the time $t = 0$ [6].

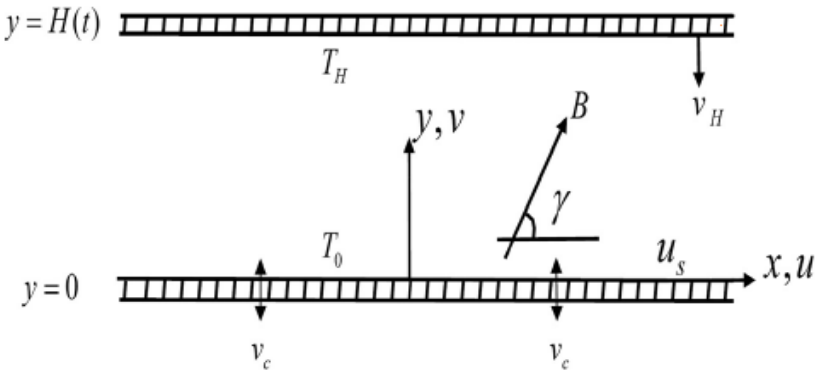

FIGURE 3.1: Geometry configuration of the problem.

The case of $\alpha > 0$ corresponds to the squeezing motion of plates, whereas $\alpha < \dfrac{1}{t}$ the plates move apart. Along the direction normal to the xy-plane, the velocity and temperature can be seen as unchanged. The Ohm's law gives the form of the current density vector $\mathbf{J}$ [43]:

$$\mathbf{J} = \sigma(\mathbf{V} \times \mathbf{B}) = (0, 0, uB_m sin\gamma, vB_m cos\gamma),$$

in which σ is the electrical conductivity, and $\mathbf{V} = (u, v, 0)$ is the velocity vector. Utilizing the above equation, we obtain the Lorentz force:

$$\mathbf{J} \times \mathbf{B} = (\sigma B_m^2 v sin\gamma cos\gamma - \sigma B_m^2 u sin^2\gamma, \sigma B_m^2 u sin\gamma cos\gamma - \sigma B_m^2 v sin\gamma cos^2\gamma, 0)\,,$$

and the joule heating:

$$\tfrac{1}{\sigma}\mathbf{J}.\mathbf{J} = \sigma B_m^2 \left(u^2 sin^2\gamma + v^2 cos^2\gamma - 2uv sin\gamma cos\gamma\right).$$

The flow is described in the presence of suction/injection, viscous dissipation and Joule heating by continuity, momentum and energy equation are as follows:

Continuity equation:

$$\frac{\partial u}{\partial x}+\frac{\partial v}{\partial y}=0. \tag{3.1}$$

Momentum equation for u-velocity:

$$\frac{\partial u}{\partial t}+u\frac{\partial u}{\partial x}+v\frac{\partial u}{\partial y}=\frac{-1}{\rho}\frac{\partial p}{\partial x}+\frac{\mu}{\rho}\left(\frac{\partial^2 u}{\partial x^2}+\frac{\partial^2 u}{\partial y^2}\right)+\frac{\sigma B_m^2}{\rho}\sin\gamma\left(v\cos\gamma-u\sin\gamma\right). \tag{3.2}$$

Momentum equation for v-velocity:

$$\frac{\partial v}{\partial t}+u\frac{\partial v}{\partial x}+v\frac{\partial v}{\partial y}=\frac{-1}{\rho}\frac{\partial p}{\partial y}+\frac{\mu}{\rho}\left(\frac{\partial^2 v}{\partial x^2}+\frac{\partial^2 v}{\partial y^2}\right)+\frac{\sigma B_m^2}{\rho}\cos\gamma\left(u\sin\gamma-v\cos\gamma\right). \tag{3.3}$$

Energy equation:

$$\frac{\partial T}{\partial t}+u\frac{\partial T}{\partial x}+v\frac{\partial T}{\partial y}=\frac{\kappa}{\rho C_p}\left(\frac{\partial^2 T}{\partial x^2}+\frac{\partial^2 T}{\partial y^2}\right)+\frac{\mu}{\rho C_p}\left[2\left(\frac{\partial u}{\partial x}\right)^2+2\left(\frac{\partial v}{\partial y}\right)^2+\left(\frac{\partial u}{\partial y}+\frac{\partial v}{\partial x}\right)^2\right]+\frac{\sigma B_m^2}{\rho C_p}\left(u\sin\gamma-v\cos\gamma\right)^2. \tag{3.4}$$

Here u and v are the velocity components of the fluid along the x and y direction, respectively. T is the temperature, μ is the total dynamic viscosity, ρ is the density, C_p is the real heat capacity of the fluid, and κ is the thermal conductivity of the fluid.

Boundary conditions executed on lower and upper plates are:

$$\left.\begin{aligned}
&u=u_s=\frac{bx}{1-\alpha t}, \qquad v=v_c=-\frac{v_0}{(1-\alpha t)^{\frac{1}{2}}},\\
&T=T_0 \qquad at \quad y=0,\\
&u=0, \qquad\quad v=v_H=\frac{dH}{dt}=-\frac{\alpha l}{2(1-\alpha t)^{\frac{1}{2}}},\\
&T=T_H=T_0+\left(\frac{T_0}{1-\alpha t}\right) \quad at \quad y=H(t).
\end{aligned}\right\} \tag{3.5}$$

Here, u_s denotes lower plate stretching velocity, v_c represents lower plate mass flux velocity, v_H denotes upper plate velocity, T_0 is lower plate surface temperature and T_H denotes upper plate surface temperature.

The following similarity transformations are used to convert partial differential

equations into set of ordinary differential equations.

$$\left.\begin{aligned} u &= \tfrac{-x}{H(t)} v_H f'(\eta), \\ v &= v_H f(\eta), \\ \theta(\eta) &= \frac{T - T_0}{T_H - T_0}, \\ \eta &= \tfrac{y}{H(t)}, \\ H(t) &= l(1-\alpha t)^{\frac{1}{2}}. \end{aligned}\right\} \tag{3.6}$$

3.3 Dimensionless Structure of the Governing Equations

Substituting (3.6) into the L.H.S of continuity equation (3.1), we get:

$$\frac{\partial\left[\frac{-x}{H(t)} v_H f'(\eta)\right]}{\partial x} + \frac{\partial\left[v_H f(\eta)\right]}{\partial y},$$

where,

$$v_H = \frac{dH}{dt} = -\frac{\alpha l}{2(1-\alpha t)^{\frac{1}{2}}} \quad \text{and} \quad \eta = \frac{y}{H(t)},$$

hence, we obtain,

$$\frac{\alpha l}{2(1-\alpha t)^{\frac{1}{2}} H(t)} f'(\eta) - \frac{\alpha l}{2(1-\alpha t)^{\frac{1}{2}} H(t)} f'(\eta) = 0.$$

Thus, the continuity equation is satisfied identically.

To convert momentum equations (3.2) and (3.3) into dimensionless form, we will first eliminate the pressure term. For this purpose, we differentiate (3.2) and (3.3) w.r.to y and x respectively. The following are some important derivatives, which will be used to convert (3.2) into the dimensionless form:

$$u = \frac{-x}{H(t)} v_H f'(\eta) = \frac{-x\eta}{y}\left(\frac{-\alpha l}{2(1-\alpha t)^{\frac{1}{2}}}\right) f'(\eta) = \frac{\alpha x}{2(1-\alpha t)} f'(\eta),$$

$$\frac{\partial u}{\partial t} = \frac{\alpha^2 x f'}{2(1-\alpha t)^2} + \frac{\alpha^2 x y f''}{4l(1-\alpha t)^{\frac{5}{2}}},$$

- $\dfrac{\partial}{\partial y}\left(\dfrac{\partial u}{\partial t}\right) = \dfrac{3\alpha^2 x f''}{4l(1-\alpha t)^{\frac{5}{2}}} + \dfrac{\alpha^2 x y f'''}{4l^2(1-\alpha t)^3}$,
  $\dfrac{\partial u}{\partial x} = \dfrac{\alpha}{2(1-\alpha t)} f'(\eta)$,
  $u\dfrac{\partial u}{\partial x} = \dfrac{\alpha^2 x f'^2}{4(1-\alpha t)^2}$,
- $\dfrac{\partial}{\partial y}\left(u\dfrac{\partial u}{\partial x}\right) = \dfrac{\alpha^2 x f' f''}{2l(1-\alpha t)^{\frac{5}{2}}}$,
  $\dfrac{\partial u}{\partial y} = \dfrac{\alpha x}{2l(1-\alpha t)^{\frac{3}{2}}} f''(\eta)$,
  $v\dfrac{\partial u}{\partial y} = \dfrac{-\alpha^2 x f f''}{4(1-\alpha t)^2}$,
- $\dfrac{\partial}{\partial y}\left(v\dfrac{\partial u}{\partial y}\right) = \dfrac{-\alpha^2 x f' f''}{4l(1-\alpha t)^{\frac{5}{2}}} - \dfrac{\alpha^2 x f f'''}{4l(1-\alpha t)^{\frac{5}{2}}}$,
  $\dfrac{\partial u}{\partial x} = 0$,
  $\dfrac{\partial^2 u}{\partial x^2} = 0$,
- $\dfrac{\partial}{\partial y}\left(\dfrac{\partial^2 u}{\partial x^2}\right) = 0$,
  $\dfrac{\partial^2 u}{\partial y^2} = \dfrac{\alpha x}{2l^2(1-\alpha t)^2} f'''(\eta)$,
- $\dfrac{\partial}{\partial y}\left(\dfrac{\partial^2 u}{\partial y^2}\right) = \dfrac{\alpha x f^{(iv)}}{2l^3(1-\alpha t)^{\frac{5}{2}}}$,
- $\dfrac{\partial}{\partial y}\left(-\dfrac{1}{\rho}\dfrac{\partial p}{\partial x}\right) = -\dfrac{1}{\rho}\dfrac{\partial^2 p}{\partial x \partial y}$,
  $\dfrac{\partial^2 u}{\partial y^2} = \dfrac{\alpha x}{2(1-\alpha t)^2}\left(\dfrac{\nu}{l^2}\right) f'''$,
  $B_m^2 = B_0^2(1-\alpha t)^{-1}, \quad \delta = \dfrac{H}{x} = \dfrac{l(1-\alpha t)^2}{x}$,
- $\dfrac{\partial}{\partial y}\left[\dfrac{\sigma B_m^2}{\rho}\sin\gamma\left(-\dfrac{\alpha l}{2(1-\alpha t)^{\frac{1}{2}}} f(\eta)\cos\gamma - \dfrac{\alpha x}{2(1-\alpha t)} f'(\eta)\sin\gamma\right)\right]$
  $= -\dfrac{\sigma B_m^2}{\rho}\dfrac{\alpha f'}{2(1-\alpha t)}\sin\gamma\cos\gamma - \dfrac{\sigma B_m^2}{\rho}\dfrac{\alpha x f''}{2l(1-\alpha t)^{\frac{3}{2}}}\sin^2\gamma.$

Using all of the derivatives calculated above in (3.2), we get:

$$\frac{3\alpha^2 x f''}{4l(1-\alpha t)^{\frac{5}{2}}} + \frac{\alpha^2 x \eta f'''}{4l(1-\alpha t)^{\frac{5}{2}}} + \frac{\alpha^2 x f' f''}{4l(1-\alpha t)^{\frac{5}{2}}} - \frac{\alpha^2 x f f'''}{4l(1-\alpha t)^{\frac{5}{2}}} - \frac{\mu}{\rho}\frac{\alpha x f^{iv}}{2l^3(1-\alpha t)^{\frac{5}{2}}}$$
$$+ \frac{\sigma B_m^2}{\rho}\frac{\alpha f'}{2(1-\alpha t)}\sin\gamma\cos\gamma + \frac{\sigma B_m^2}{\rho}\frac{\alpha x f''}{2l(1-\alpha t)^{\frac{3}{2}}}\sin^2\gamma = -\frac{1}{\rho}\frac{\partial^2 p}{\partial x \partial y}. \tag{3.7}$$

The following derivatives are necessary, when we differentiate (3.3) w.r.to x,

$$v = v_H f(\eta) = -\frac{\alpha l}{2(1-\alpha t)^{\frac{1}{2}}} f(\eta),$$

$$\frac{\partial v}{\partial t} = -\frac{\alpha^2 l f}{4(1-\alpha)^{\frac{3}{2}}} - \frac{\alpha^2 y f'}{4(1-\alpha t)^2},$$

- $\dfrac{\partial}{\partial x}\left(\dfrac{\partial v}{\partial t}\right) = 0,$

$$\frac{\partial v}{\partial x} = 0,$$

$$u\frac{\partial v}{\partial x} = 0,$$

- $\dfrac{\partial}{\partial x}\left(u\dfrac{\partial v}{\partial x}\right) = 0,$

$$\frac{\partial v}{\partial y} = -\frac{\alpha f'}{2(1-\alpha t)},$$

$$v\frac{\partial v}{\partial y} = \frac{\alpha^2 l f f'}{4(1-\alpha t)^{\frac{3}{2}}},$$

- $\dfrac{\partial}{\partial x}\left(v\dfrac{\partial v}{\partial y}\right) = 0,$

$$\frac{\partial v}{\partial x} = 0,$$

$$\frac{\partial^2 v}{\partial x^2} = 0,$$

- $\dfrac{\partial}{\partial x}\left(\dfrac{\partial^2 v}{\partial x^2}\right) = 0,$

$$\frac{\partial^2 v}{\partial y^2} = -\frac{\alpha f''}{2l(1-\alpha t)^{\frac{3}{2}}},$$

- $\dfrac{\partial}{\partial x}\left(\dfrac{\partial^2 v}{\partial y^2}\right) = 0,$
- $\dfrac{\partial}{\partial x}\left(-\dfrac{1}{\rho}\dfrac{\partial p}{\partial y}\right) = -\dfrac{1}{\rho}\dfrac{\partial^2 p}{\partial x \partial y}$
- $\dfrac{\partial}{\partial x}\left[\dfrac{\sigma B_m^2}{\rho}\cos\gamma\left(\dfrac{\alpha x f'}{2(1-\alpha t)}\sin\gamma + \dfrac{\alpha l f}{2(1-\alpha t)^{\frac{1}{2}}}\cos\gamma\right)\right] = \dfrac{\sigma B_m^2}{\rho}\dfrac{\alpha f'\sin\gamma\cos\gamma}{2(1-\alpha t)}.$

Using all of the derivatives calculated above in (3.3), we get:

$$-\frac{\sigma B_m^2}{\rho}\frac{\alpha f'}{2(1-\alpha t)}\sin\gamma\cos\gamma = -\frac{1}{\rho}\frac{\partial^2 p}{\partial x \partial y}. \tag{3.8}$$

For the elimination of pressure term equating (3.7) and (3.8), we get:

$$\frac{\mu}{\rho}\frac{\alpha x f^{(iv)}}{2l^3(1-\alpha t)^{\frac{5}{2}}}-\frac{\alpha^2 x\eta f'''}{4l(1-\alpha t)^{\frac{5}{2}}}-\frac{3\alpha^2 x f''}{4l(1-\alpha t)^{\frac{5}{2}}}-\frac{\alpha^2 x f' f''}{4l(1-\alpha t)^{\frac{5}{2}}}+\frac{\alpha^2 x f f'''}{4l(1-\alpha t)^{\frac{5}{2}}}-\frac{\sigma B_m^2}{\rho}$$
$$\frac{\alpha f'}{2(1-\alpha t)}\sin\gamma\cos\gamma-\frac{\sigma B_m^2}{\rho}\frac{\alpha x f''}{2l(1-\alpha t)^{\frac{3}{2}}}\sin^2\gamma-\frac{\sigma B_m^2}{\rho}\frac{\alpha f'}{2(1-\alpha t)}\sin\gamma\cos\gamma=0.$$

Dividing the above equation by $\frac{\rho}{\mu}\frac{2l^3(1-\alpha t)^{\frac{5}{2}}}{\alpha x}$, yields,

$$f^{(iv)}-\frac{\rho l^2\alpha\eta f'''}{2\mu}-\frac{3\rho l^2\alpha f''}{2\mu}-\frac{\rho l^2\alpha f' f''}{2\mu}+\frac{\rho l^2\alpha f f'''}{2\mu}-\frac{2\sigma B_m^2 l^3(1-\alpha t)^{\frac{3}{2}}f'}{\mu x}$$
$$\sin\gamma\cos\gamma-\frac{\sigma B_m^2 l^2(1-\alpha t)f''}{\mu}\sin^2\gamma=0,$$
$$\Rightarrow\quad f^{(iv)}-\frac{\rho l^2\alpha}{2\mu}\left(\eta f'''+3f''+f'f''-ff'''\right)-\frac{\sigma B_0 l^2}{\mu}$$
$$\sin\gamma\left(\sin\gamma f''+2\delta\cos\gamma f'\right)=0,$$

where,

$$B_m^2=B_0^2(1-\alpha t)^{-1},\quad M^2=\frac{\sigma B_0^2 l^2}{\rho\nu},\quad S=\frac{\alpha l^2}{2\nu}.$$

Finally, the dimensionless form of (3.2) and (3.3):

$$f^{(iv)}-S\left(\eta f'''+3f''+f'f''-ff'''\right)-M^2\sin\gamma\left(\sin\gamma f''+2\delta\cos\gamma f'\right)=0.$$

For the conversion of the temperature equation (3.4) into an ordinary differential equation. The following derivatives are evaluated:

$$T=\theta(\eta)\left(\frac{T_0}{1-\alpha t}\right)+T_0,\qquad \frac{\partial T}{\partial t}=\frac{T_0\alpha y}{2l(1-\alpha t)^{\frac{5}{2}}}\theta'+\frac{T_0\alpha}{(1-\alpha t)^2}\theta,$$
$$u\frac{\partial T}{\partial x}=0,\qquad \frac{\partial T}{\partial y}=\frac{T_0}{l(1-\alpha t)^{\frac{3}{2}}}\theta',$$
$$\frac{\partial^2 T}{\partial y^2}=\frac{T_0}{l^2(1-\alpha t)^2}\theta'',\qquad v\frac{\partial T}{\partial y}=-\frac{T_0\alpha}{2(1-\alpha t)^2}f\theta',$$
$$\frac{\partial u}{\partial x}=\frac{\alpha f'}{2(1-\alpha t)},\qquad \frac{\partial v}{\partial y}=-\frac{\alpha f'}{2(1-\alpha t)},$$
$$\frac{\partial u}{\partial y}=\frac{\alpha x f''}{2l(1-\alpha t)^{\frac{3}{2}}},\qquad \frac{\partial v}{\partial x}=0,$$
$$u\frac{\partial T}{\partial x}=0,\qquad \frac{\partial T}{\partial y}=\frac{T_0}{l(1-\alpha t)^{\frac{3}{2}}}\theta',$$

Using the above derivatives into (3.4), to get:

$$\frac{T_0\alpha y}{2l(1-\alpha t)^{\frac{5}{2}}}\theta' + \frac{T_0\alpha}{(1-\alpha t)^2}\theta - \frac{T_0\alpha}{2(1-\alpha t)^2}f\theta' = \frac{\kappa}{\rho C_p}\left(\frac{T_0}{l^2(1-\alpha t)^2}\theta''\right) + \frac{\mu}{\rho C_p}$$
$$\left(\frac{\alpha^2x^2f''^2}{4l^2(1-\alpha t)^3} + \frac{\alpha^2f'^2}{(1-\alpha t)^2}\right) + \frac{\sigma B_0^2}{\rho C_p(1-\alpha t)}\left(\frac{\alpha x f'\sin\gamma}{2(1-\alpha t)} + \frac{\alpha l f\cos\gamma}{2(1-\alpha t)^{\frac{1}{2}}}\right)^2,$$

$$\Rightarrow \quad \frac{T_0\alpha\eta}{2(1-\alpha t)^2}\theta' + \frac{T_0\alpha}{(1-\alpha t)^2}\theta - \frac{T_0\alpha}{2(1-\alpha t)^2}f\theta' = \frac{\kappa}{(\rho C_p)}\left(\frac{T_0}{l^2(1-\alpha t)^2}\theta''\right)$$
$$+\frac{\mu}{(\rho C_p)}\left(\frac{\alpha^2x^2f''^2}{4l^2(1-\alpha t)^3} + \frac{\alpha^2f'^2}{(1-\alpha t)^2}\right) + \frac{\sigma B_0^2}{(\rho C_p)(1-\alpha t)}$$
$$\left(\frac{\alpha^2x^2f'^2}{4(1-\alpha t)^2}\sin^2\gamma + \frac{\alpha^2l^2f^2}{4(1-\alpha t)}\cos^2\gamma + \frac{2\alpha_2 xlff'}{4(1-\alpha t)^{\frac{3}{2}}}\sin\gamma\cos\gamma\right),$$

$$\Rightarrow \quad \frac{T_0\alpha}{2(1-\alpha t)^2}(\eta\theta' + 2\theta - f\theta') = \frac{1}{C_p(1-\alpha t)^2}\frac{\kappa T_0}{\rho l^2}\theta'' + \frac{1}{C_p(1-\alpha t)}\frac{\nu\alpha^2x^2}{4l^2(1-\alpha t)^2}$$
$$\left(f''^2 + 4\delta^2f'^2\right) + \frac{1}{C_p(1-\alpha t)}\frac{\sigma B_0^2}{\rho}\frac{\alpha^2x^2}{4(1-\alpha t)^2}\left(f'^2\sin^2\gamma + \delta^2f^2\cos^2\gamma\right.$$
$$\left.+2\delta ff'\sin\gamma\cos\gamma\right),$$

$$\Rightarrow \quad \frac{T_0\alpha}{2(1-\alpha t)^2}(\eta\theta' + 2\theta - f\theta') = \frac{1}{C_p(1-\alpha t)^2}\left[\frac{\kappa T_0}{\rho l^2}\theta'' + \frac{\nu\alpha^2x^2}{4l^2(1-\alpha t)}\left(f''^2\right.\right.$$
$$\left.\left.+4\delta^2f'^2\right) + \frac{\sigma B_0^2\alpha^2x^2}{4\rho(1-\alpha t)}\left(f'^2\sin^2\gamma + \delta^2f^2\cos^2\gamma + 2\delta ff'\sin\gamma\cos\gamma\right)\right],$$

$$\Rightarrow \quad \frac{T_0\alpha}{2}(\eta\theta' + 2\theta - f\theta') = \frac{\nu}{C_pl^2}\left[\frac{\kappa T_0}{\rho\nu}\theta'' + \frac{\alpha^2x^2}{4(1-\alpha t)}\left(f''^2 + 4\delta^2f'^2\right)\right.$$
$$\left.+\frac{\sigma B_0^2l^2\alpha^2x^2}{\rho\nu 4(1-\alpha t)}\left(f'^2\sin^2\gamma + \delta^2f^2\cos^2\gamma + 2\delta ff'\sin\gamma\cos\gamma\right)\right],$$

$$\Rightarrow \quad \frac{T_0\alpha}{2}(\eta\theta' + 2\theta - f\theta') = \frac{\nu}{C_pl^2}\left[\frac{\kappa T_0}{\rho\nu}\theta'' + \frac{\alpha^2x^2}{4(1-\alpha t)}\left(f''^2 + 4\delta^2f'^2\right)\right.$$
$$\left.+M^2\frac{\alpha^2x^2}{4(1-\alpha t)}\left(f'^2\sin^2\gamma + \delta^2f^2\cos^2\gamma + 2\delta ff'\sin\gamma\cos\gamma\right)\right],$$

$$\Rightarrow \quad \frac{T_0\alpha}{2}(\eta\theta' + 2\theta - f\theta') = \frac{\nu}{C_pl^2}\frac{\alpha^2x^2}{4(1-\alpha t)}\left[\frac{4(1-\alpha t)}{\alpha^2x^2}\frac{\kappa T_0}{\rho\nu}\theta'' + f''^2 + 4\delta^2f'^2\right.$$
$$\left.+M^2\left(f'^2\sin^2\gamma + \delta^2f^2\cos^2\gamma + 2\delta ff'\sin\gamma\cos\gamma\right)\right],$$

$$\Rightarrow \quad \frac{2T_0C_pl^2(1-\alpha t)}{\nu\alpha x^2}(\eta\theta' + 2\theta - f\theta') = \frac{4(1-\alpha t)}{\alpha^2x^2}\frac{\kappa T_0}{\rho\nu}\theta'' + f''^2 + 4\delta^2f'^2$$
$$+M^2\left(f'^2\sin^2\gamma + \delta^2f^2\cos^2\gamma + 2\delta ff'\sin\gamma\cos\gamma\right),$$

$$\Rightarrow \quad \frac{2T_0C_pl^2(1-\alpha t)}{\nu\alpha x^2}(\eta\theta' + 2\theta - f\theta') = \frac{4(1-\alpha t)}{\alpha^2x^2}\frac{\kappa T_0}{\rho\nu}\left[\theta'' + \frac{\rho\nu\alpha^2x^2}{\kappa T_0 4(1-\alpha t)}\left(f''^2\right.\right.$$
$$\left.\left.+4\delta^2f'^2\right) + \frac{\rho\nu\alpha^2x^2}{\kappa T_0 4(1-\alpha t)}M^2\left(f'^2\sin^2\gamma + \delta^2f^2\cos^2\gamma + 2\delta ff'\sin\gamma\cos\gamma\right)\right],$$

$$
\begin{aligned}
\Rightarrow \quad & \frac{\mu C_p \alpha l^2}{2\nu\kappa}\left(\eta\theta' + 2\theta - f\theta'\right) = \theta'' + \frac{\rho\nu\alpha^2 x^2}{\kappa T_0 4(1-\alpha t)}\left(f''^2 + 4\delta^2 f'^2\right) \\
& + \frac{\rho\nu\alpha^2 x^2}{\kappa T_0 4(1-\alpha t)} M^2\left(f'^2\sin^2\gamma + \delta^2 f^2\cos^2\gamma + 2\delta f f'\sin\gamma\cos\gamma\right), \\
\Rightarrow \quad & \frac{\mu C_p \alpha l^2}{2\nu\kappa}\left(\eta\theta' + 2\theta - f\theta'\right) = \theta'' + \frac{\rho\nu\alpha^2 x^2}{\kappa T_0 4(1-\alpha t)}\Big[f''^2 + 4\delta^2 f'^2 \\
& + M^2\left(f'^2\sin^2\gamma + \delta^2 f^2\cos^2\gamma + 2\delta f f'\sin\gamma\cos\gamma\right)\Big], \\
\Rightarrow \quad & \theta'' + \frac{\mu C_p \alpha l^2}{2\nu\kappa}\left(f\theta' - \eta\theta' - 2\theta\right) + \frac{\rho\nu\alpha^2 x^2}{\kappa T_0 4(1-\alpha t)}\Big[f''^2 + 4\delta^2 f'^2 \\
& + M^2\left(f'^2\sin^2\gamma + \delta^2 f^2\cos^2\gamma + 2\delta f f'\sin\gamma\cos\gamma\right)\Big] = 0,
\end{aligned}
$$

where,

$$
\begin{aligned}
Pr &= \frac{\mu C_p}{\kappa}, & S &= \frac{\alpha l^2}{2\nu}, \\
E_c &= \frac{u_0^2}{C_p R^2 (T_H - T_0)}, & R &= \frac{u_0\delta}{v_H}, \\
u_0 &= \frac{bx}{1-\alpha t}, & v_H &= -\frac{\alpha l}{2(1-\alpha t)^{\frac{1}{2}}}, \\
T_H - T_0 &= \frac{T_0}{1-\alpha t}, & S_b &= \frac{2v_0}{\alpha l}, \\
\frac{\mu\alpha^2 x^2 C_p}{4\kappa C_p T_0}(1-\alpha t) &= \frac{\mu C_p}{\kappa}\frac{\alpha^2 x^2}{4C_p T_0(1-\alpha t)} \\
&= Pr\frac{\alpha^2 x^2 u_0^2 \delta^2}{4C_p T_0(1-\alpha t)R^2 v_H^2} \\
&= Pr\frac{b^2 x^2}{C_p T_0(1-\alpha t)R^2} \\
&= Pr\frac{b^2 x^2}{C_p(T_H - T_0)(1-\alpha t)^2 R^2} \\
&= \frac{P_r}{C_p(T_H - T_0)R^2}\frac{b^2 x^2}{(1-\alpha t)^2} \\
&= \frac{P_r u_0^2}{C_p(T_H - T_0)R^2} = PrE_c.
\end{aligned}
$$

Finally, the dimensionless form of (3.4):

$$
\begin{aligned}
& \theta'' + PrS\left(f\theta' - \eta\theta' - 2\theta\right) + PrE_c\Big[f''^2 + 4\delta^2 f'^2 \\
& + M^2\left(f'^2\sin^2\gamma + \delta^2 f^2\cos^2\gamma + 2\delta f f'\sin\gamma\cos\gamma\right)\Big] = 0.
\end{aligned}
$$

The following procedures have now been taken to transform the corresponding boundary conditions into the dimensionless form:

- $u = u_s \quad at \quad y = 0,$

  $$-\frac{x}{H(t)} v_H f'(\eta) = u_s \quad at \quad \eta = 0,$$

  $$f'(\eta) = \frac{u_s H(t)}{-x v_H},$$

  $$f'(0) = \frac{u_s \delta}{v_H},$$

  $$f'(0) = R.$$

- $v = -\dfrac{v_0}{(1-\alpha t)^{\frac{1}{2}}} \quad at \quad y = 0,$

  $$v_H f(\eta) = -\frac{v_0}{(1-\alpha t)^{\frac{1}{2}}} \quad at \quad \eta = 0,$$

  $$f(0) = \frac{2v_0}{\alpha l},$$

  $$f(0) = S_b.$$

- $T = T_0 \quad at \quad y = 0,$

  $$\theta(\eta)\left(\frac{T_0}{1-\alpha t}\right) + T_0 = T_0 \quad at \quad \eta = 0,$$

  $$\theta(0) = \left(\frac{T_0}{1-\alpha t}\right) = 0,$$

  $$\theta(0) = 0.$$

- $u = 0 \quad at \quad y = H(t),$

  $$-\frac{x}{H(t)} v_H f'(\eta) = 0 \quad at \quad \eta = 1,$$

  $$f'(1) = 0.$$

- $v = v_H \quad at \quad y = H(t),$

  $$v_H f(\eta) = v_H \quad at \quad \eta = 1,$$

  $$f(1) = 1.$$

- $T = T_0 + \dfrac{T_0}{1-\alpha t} \quad at \quad y = H(t),$

  $$\theta(\eta)\left(\frac{T_0}{1-\alpha t}\right) + T_0 = T_0 + \frac{T_0}{1-\alpha t} \quad at \quad \eta = 1,$$

  $$\theta(1) = \left(\frac{T_0}{1-\alpha t}\right) = \frac{T_0}{1-\alpha t} = 1.$$

Hence, we get the following set of ordinary differential equations:

$$f^{(iv)} - S\left(\eta f''' + 3f'' + f'f'' - ff'''\right) - M^2 \sin\gamma \left(\sin\gamma f'' + 2\delta\cos\gamma f'\right) = 0, \quad (3.9)$$

$$\begin{aligned}\theta'' + PrS\left(f\theta' - \eta\theta' - 2\theta\right) + PrE_c\Big[f''^2 + 4\delta^2 f'^2 \\ + M^2\left(f'^2\sin^2\gamma + \delta^2 f^2\cos^2\gamma + 2\delta f f'\sin\gamma\cos\gamma\right)\Big] = 0,\end{aligned} \quad (3.10)$$

subject to boundary conditions:

$$\left.\begin{aligned} f(0) = S_b, \quad f'(0) = R, \quad \theta(0) = 0, \\ f(1) = 1, \quad f'(1) = 0, \quad \theta(1) = 1, \end{aligned}\right\} \quad (3.11)$$

where S is the squeezing number, Pr is the prandtl number, M is the magnetic parameter, E_c is the Eckert number and R is the lower plate stretching parameter. The lower plate suction/injection is denoted by S_b with $S_b < 0$ for injection and $S_b > 0$ for suction.

Before going toward the mathematical solution, the skin friction coefficient C_f or the shear stress and the Nusselt number Nu or heat transfer coefficient on the lower plate surface are represented as:

$$C_f = \frac{\mu\left(\frac{\partial u}{\partial y}\right)_{y=H(t)}}{v_H^2\rho},$$
$$Nu = \frac{l\left(\frac{\partial T}{\partial y}\right)_{y=H(t)}}{T_H - T_0}.$$

The following steps elaborate the conversion of C_f and Nu into dimensionless form:

$$C_f = -\frac{\mu x v_H}{\rho v_H^2 l^2(1-\alpha t)} f''(\eta) = -\frac{\mu x}{\rho v_H l^2(1-\alpha t)} f''(\eta),$$
$$C_f = -\frac{\mu x}{\rho\left(\frac{-\alpha l}{2(1-\alpha t)^{\frac{1}{2}}}\right) l^2(1-\alpha t)} f''(\eta),$$

$$C_f = -\frac{2\mu x}{\rho\alpha l^3(1-\alpha t)^{\frac{1}{2}}} f''(\eta),$$

$$f''(\eta) = \frac{\rho\alpha l^3(1-\alpha t)^{\frac{1}{2}}}{\mu x} C_f, \quad \text{where} \quad y = H(t) \quad \text{and} \quad \eta = 1,$$

$$f''(1) = \frac{\rho\alpha l^3(1-\alpha t)^{\frac{1}{2}}}{\nu\rho x} C_f = \frac{\alpha l^3(1-\alpha t)^{\frac{1}{2}}}{\frac{u_s x}{Re_x} x} C_f,$$

$$f''(1) = \frac{\alpha l^3(1-\alpha t)^{\frac{1}{2}}}{u_s x^2} Re_x C_f,$$

$$f''(1) = \frac{\alpha l^3(1-\alpha t)^{\frac{1}{2}}}{\frac{bx}{(1-\alpha t)} x^2} Re_x C_f,$$

$$f''(1) = \frac{\alpha l^3(1-\alpha t)^{\frac{3}{2}}}{bx^3} Re_x C_f.$$

Now,

$$Nu = \frac{l\left(\frac{\partial T}{\partial y}\right)_{y=H(t)}}{T_H - T_0},$$

$$Nu = \frac{l}{T_H - T_0} \frac{T_0}{l(1-\alpha t)^{\frac{3}{2}}} \theta'(\eta),$$

$$Nu = \frac{l}{(T_H - T_0)} \frac{(T_H - T_0)(1-\alpha t)}{l(1-\alpha t)^{\frac{3}{2}}}, \quad \text{where} \quad T_H = T_0 + \frac{T_0}{(1-\alpha t)} \theta'(\eta),$$

$$Nu = \frac{(1-\alpha t)}{(1-\alpha t)^{\frac{1}{2}}} \theta'(\eta),$$

$$\theta'(1) = (1-\alpha t)^{\frac{1}{2}} Nu, \quad \text{where} \quad y = H(t) \quad \text{at} \quad \eta = 1,$$

$$\theta'(1) = \left(\frac{bx}{u_s}\right)^{\frac{1}{2}} Nu,$$

$$\theta'(1) = \frac{(bx)^{\frac{1}{2}}}{\left(\frac{\nu Re_x}{x}\right)^{\frac{1}{2}}} Nu.$$

Here Re_x represent the local Reynolds number which is used to categorized the flow pattern.

3.4 Numerical Treatment

This section is dedicated to the implementation of the shooting method to solve the transformed ODEs (3.9) and (3.10) subject to the boundary conditions (3.11). One can easily observe that (3.9) independent of θ, so we will first find the solution

of (3.9). For this purpose, the following notations are used:

$$\begin{aligned} f &= g_1, \\ f' &= g_1' = g_2, \\ f'' &= g_2' = g_3, \\ f''' &= g_3' = g_4, \\ f^{(iv)} &= g_4'. \end{aligned}$$

Utilizing the above notations, we have the following system of four first order differential equations:

$$\left.\begin{aligned} &g_1' = g_2; && g_1(0) = S_b = \frac{2v_0}{\alpha l}, \\ &g_2' = g_3; && g_2(0) = R = \frac{u_s \delta}{v_H}, \\ &g_3' = g_4; && g_3(0) = \alpha_1, \\ &g_4' = S(3g_3 + \eta g_4 + g_2 g_3 - g_1 g_4) && \\ &+M^2 \sin\gamma(2\delta\cos\gamma g_2 + \sin\gamma g_2); && g_4(0) = \alpha_2. \end{aligned}\right\} \tag{3.12}$$

To solve the above system by using Runge Kutta method of order four, two missing initial conditions are assumed to be α_1 and α_2, such that:

$$\begin{aligned} g_1(\eta, \alpha_1, \alpha_2)_{\eta=1} - 1 &= 0, \\ g_2(\eta, \alpha_1, \alpha_2)_{\eta=1} - 0 &= 0. \end{aligned}$$

These non-linear algebraic equations are solved for α_1 and α_2 by Newton's method which has the following iterative scheme:

$$\begin{bmatrix} u^{n+1} \\ v^{n+1} \end{bmatrix} = \begin{bmatrix} u^n \\ v^n \end{bmatrix} - \begin{bmatrix} \frac{\partial g_1}{\partial \alpha_1} & \frac{\partial g_1}{\partial \alpha_2} \\ \frac{\partial g_2}{\partial \alpha_1} & \frac{\partial g_2}{\partial \alpha_2} \end{bmatrix}^{-1} \begin{bmatrix} g_1(\alpha_1, \alpha_2) - 1 \\ g_2(\alpha_1, \alpha_2) - 0 \end{bmatrix}. \tag{3.13}$$

To incorporate the above formula, we further need the following derivatives:

$$\frac{\partial g_1}{\partial \alpha_1} = g_5, \qquad \frac{\partial g_2}{\partial \alpha_1} = g_6, \qquad \frac{\partial g_3}{\partial \alpha_1} = g_7, \qquad \frac{\partial g_4}{\partial \alpha_1} = g_8,$$

$$\frac{\partial g_1}{\partial \alpha_2} = g_9, \qquad \frac{\partial g_2}{\partial \alpha_2} = g_{10}, \qquad \frac{\partial g_3}{\partial \alpha_2} = g_{11}, \qquad \frac{\partial g_4}{\partial \alpha_2} = g_{12}.$$

As the result of these notations, the Newton's iterative scheme gets the form:

$$\begin{bmatrix} u^{n+1} \\ v^{n+1} \end{bmatrix} = \begin{bmatrix} u^n \\ v^n \end{bmatrix} - \begin{bmatrix} g_5 & g_9 \\ g_6 & g_{10} \end{bmatrix}^{-1} \begin{bmatrix} g_1(\alpha_1, \alpha_2) - 1 \\ g_2(\alpha_1, \alpha_2) - 0 \end{bmatrix}. \tag{3.14}$$

In order to achieve the numerical solution, we further differentiate the ordinary differential equation (3.2) w.r.to α_1 and α_2. Hence, the following system of twelve first order coupled differential equation is achieved with initial values.

$$\begin{aligned}
&g_1' = g_2; && g_1(0) = S_b = \frac{2v_0}{\alpha l},\\
&g_2' = g_3; && g_2(0) = R = \frac{u_s \delta}{v_H},\\
&g_3' = g_4; && g_3(0) = \alpha_1,\\
&g_4' = S(3g_3 + \eta g_4 + g_2 g_3 - g_1 g_4) && \\
&+ M^2 \sin\gamma(2\delta \cos\gamma g_2 + \sin\gamma g_2); && g_4(0) = \alpha_2,\\
&g_5' = g_6; && g_5(0) = 0,\\
&g_6' = g_7; && g_6(0) = 0,\\
&g_7' = g_8; && g_7(0) = 1,\\
&g_8' = S(3g_7 + \eta g_8 + g_6 g_3 - g_5 g_4 + g_2 g_7 - g_1 g_8) && \\
&+ M^2 \sin\gamma(2\delta \cos\gamma g_6 + \sin\gamma g_7); && g_8(0) = 0,\\
&g_9' = g_{10}; && g_9(0) = 0,\\
&g_{10}' = g_{11}; && g_{10}(0) = 0,\\
&g_{11}' = g_{12}; && g_{11}(0) = 0,\\
&g_{12}' = S(3g_{11} + \eta g_{12} + g_{10} g_3 - g_9 g_4 + g_2 g_{11} - g_1 g_{12}) && \\
&+ M^2 \sin\gamma(2\delta \cos\gamma g_{10} + \sin\gamma g_{11}); && g_{12}(0) = 1.
\end{aligned}$$

The Runge Kutta method of order four is used to solve the above initial value problem, where α_1 and α_2 are unknown initial conditions. The iterative process

is repeated until the criteria listed below is met:

$$\max\left[\mid g_1(\eta,\alpha_1,\alpha_2)-1\mid,\mid g_2(\eta,\alpha_1,\alpha_2)\mid\right]<\epsilon,$$

for an arbitrarily small positive value of ϵ. Throughout this chapter ϵ has been taken as $(10)^{-6}$.

Since (3.9) and (3.10) are coupled equations. So (3.10) will be solved separately by incorporating the solution of (3.9). For this purpose let us denote:

$$\theta = Y_1, \qquad \theta' = Y_1' = Y_2, \qquad \theta'' = Y_2',$$

to get the following first order ODE's.

$$\left.\begin{aligned} &Y_1' = Y_2; && Y_1(0)=0,\\ &Y_2' = -\Big[P_rS\left(fY_2-\eta Y_2-2Y_1\right)+P_rE_c\left\{f''^2+4\delta^2f'^2\right.\\ &\left.+M^2\left(f'^2\sin^2\gamma+f^2\delta^2\cos^2\gamma+2\delta ff'\cos\gamma\sin\gamma\right)\right\}\Big]; && Y_2(0)=m. \end{aligned}\right\} \tag{3.15}$$

The above IVP is solved numerically by Runge Kutta method of order four. In the above initial value problem, the missing condition m is to be chosen such that:

$$Y_1(\eta,m)_{\eta=1}-1=0. \tag{3.16}$$

To solve the above algebraic equation (3.16) the Newton's method is used which has the following iterative scheme:

$$m^{n+1}=m^n-\left(\frac{\partial Y_1}{\partial m}\right)^{-1}\left(Y_1(\eta,m^n)_{\eta=1}-1\right).$$

Further considering the following derivatives:

$$\frac{\partial Y_1}{\partial m}=Y_3, \qquad \frac{\partial Y_2}{\partial m}=Y_4,$$

to formulate the following Newton's iterative scheme:

$$m^{n+1}=m^n-\left[Y_3(\eta,m^n)_{\eta=1}\right]^{-1}\left(Y_1(\eta,m^n)_{\eta=1}-1\right). \tag{3.17}$$

Here n is the number of iterations ($n = 0, 1, 2, 3, 4, 5, ...$).

To incorporate the new derivative Y_3 and Y_4 system (3.15) is further differentiated w.r.to m, to get the following IVP:

$$\begin{aligned}
&Y_1' = Y_2; && Y_1(0) = 0,\\
&Y_2' = -\Big[P_r S\left(fY_2 - \eta Y_2 - 2Y_1\right) + P_r E_c \Big\{f''^2 + 4\delta^2 f'^2\\
&\quad + M^2\left(f'^2 \sin^2\gamma + f^2\delta^2\cos^2\gamma + 2\delta f f'\cos\gamma\sin\gamma\right)\Big\}\Big]; && Y_2(0) = m,\\
&Y_3' = Y_4; && Y_3(0) = 0,\\
&Y_4' = -P_r S\left(fY_4 - \eta Y_4 - 2Y_3\right); && Y_4(0) = 1.
\end{aligned}$$

The Runge Kutta method of order four has been used to solve the IVP consisting of the above four ODE's for some suitable choices of m. The missing condition m is updated by using Newton's scheme (3.17). If the following criterion is fulfilled the iterative process is stopped:

$$|Y_1(\eta, m) - 1| < \epsilon,$$

for an arbitrarily small positive value of ϵ.

3.5 Results and Discussion

In this section, the numerical results are displayed graphically to perceive the physical properties of flow more transparently. The variation in the velocity and temperature profiles are represented with graphs by varying the parameters such as the angle of inclination, the magnetic parameter, the squeeze number, the Eckert number and the parameter of the lower plate suction/injection.

Figure 3.2 and Figure 4.2 displays the impact of the squeeze number S on the velocity $f'(\eta)$ and temperature $\theta(\eta)$ respectively. Figure 3.2 shows that the velocity sharing of fluid in the regions near the upper or lower plates decrease due to increase in the value of the squeeze number. Although an opposite trend is noticed for the velocity of fluid near the central region of the plates. Figure 4.2

indicates that a increase in S causes a decrease in fluid temperature between parallel plates.

Figure 3.4 and Figure 3.5 demonstrate the velocity and temperature profile of the fluid with different magnetic parameter values. From Figure 3.4, it is noticed that at a particular time, arising magnetic parameter causes the fluid velocity to a very slight increase in regions near to the upper or lower plates, while the fluid velocity in the central region indicates an obvious decrease. The fluid at the central area has a higher velocity relative to the fluid near to plates and it is due to high Lorentz force. The Lorentz force gives a conflict in the motion of fluid. It is seen from Figure 3.5 that the temperature increases with magnetic parameter rise. Moreover, the temperature of the fluid monotonically increases from the lower to the upper plate area while the parameter of the magnetic field is small. The fluid temperature achieves maximum value for larger magnetic parameter values not on the upper plate area but at the central area of the plates. However, stronger magnetic fields naturally influence the temperature distribution. This is mostly due to corresponding changes in joule heating and the heat caused by the fluid friction with the increment in applied magnetic field. The effect of the friction forces of fluid is increased by Lorentz force in the presence of the magnetic field. Moreover, the larger friction resistances create more heat in fluid with magnetic field increasing.

Figure 3.6 and Figure 3.7 represent the velocity and temperature behaviors by rising the inclination angle of the magnetic field applied. The angles of magnetic inclination varies from 0 to $\pi/2$. Both figures depicts the same behavior for velocity and temperature profile, when they are compared for various value of magnetic parameter. The influence of the inclination angle on both fluid temperature and velocity profile is similar to those of the magnetic parameters.

Figure 3.8 and Figure 3.9 illustrate the impact of stretching parameter on dimensionless velocity of stretching parameter and temperature of the lower surface, respectively. From Figure 3.8, we conclude that the fluid velocity near the lower plate rises in order to increasing the value of the lower plate stretching function while the velocity of the fluid near the upper plate decreases. Since the parameter

for lower plate stretching is increasing gradually, the fluid with the maximum velocity does not appear in the central area between the plates, but at the surface of the lower plate. Figure 3.9 shows that the increasing lower plate stretching causes the temperature of fluid near the lower plate initially decrease and then increase. But the temperature of fluid near the upper plate lowers with greater lower plate stretching parameter.

Figure 3.10 and Figure 3.11 illustrate the effect of the lower plate suction/injection parameter on the profiles of the velocity profile and temperature profile, respectively. Figure 3.10 indicates that with increase in the lower plate injection/suction parameter, the velocity profile falls. The fluid having peak velocity does not occur in the central area when extending the lower plate for stronger suction through the lower plate and the velocity of the fluid monotonically decreases from the surface of the lower plate to the upper plate. Temperature profile decrease as the injection/suction parameter increases. It is found that the fluid having largest temperature appears at the central section within the two plates but not on the surface of upper plate when the injection/suction parameter S_b falls.

From Figure 3.12 it can be observed that temperature increases with the increase in Eckert number. This is due to viscous dissipation and Joule heating. The temperature increase significantly between the plates. Figure 3.12 also indicates that the uppermost fluid temperature for the larger Eckert number appears in the central section of the two plates and for the smaller Eckert number it appears at the surface of the upper plate.

In Figure 3.13 and Figure 3.14 the effects of squeeze number and the magnetic inclination angle on the skin friction coefficient and the Nusselt number are showed, where the magnetic inclination angle varies from 0 to $\pi/2$, respectively. It can be found that the Nusselt number is decreasing function of the magnetic inclination angle but on contrary that the total value of skin friction coefficient is an rising function. Moreover, the squeeze number enhancement causes an increment in the total value of skin friction coefficient and Nusselt number to arise for same fixed inclination angle.

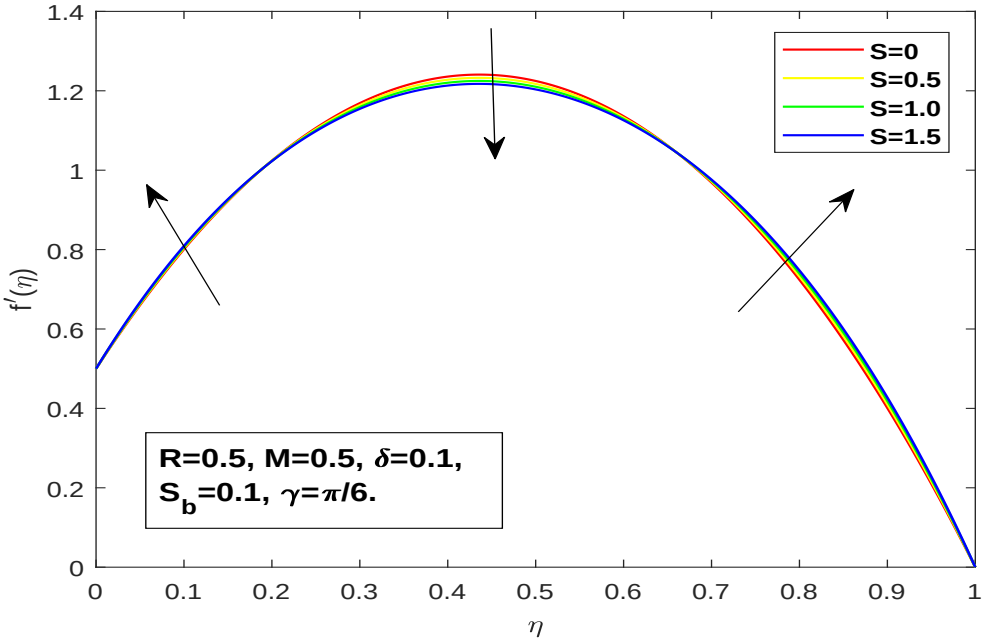

FIGURE 3.2: Impact of the squeeze number S on the longitudinal velocity profile.

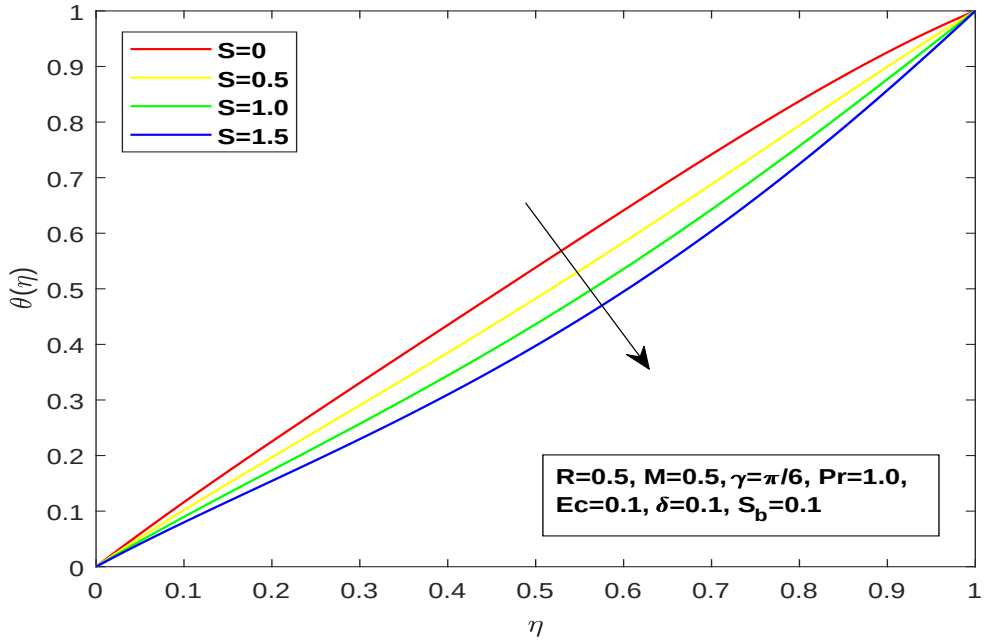

FIGURE 3.3: Impact of the squeeze number S on the temperature profile.

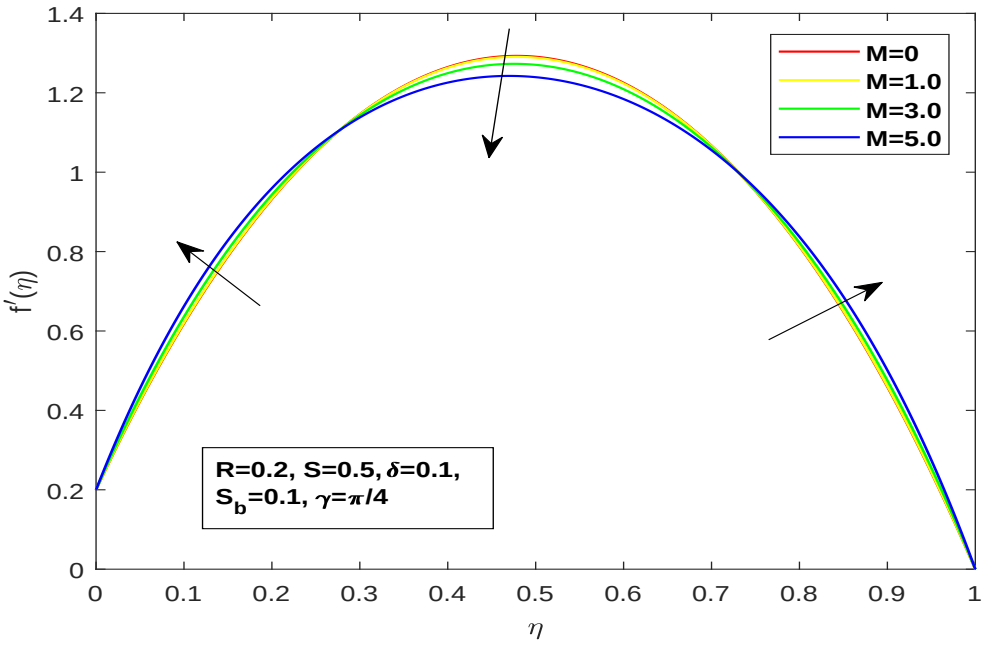

FIGURE 3.4: Impact of the magnetic parameter M on the longitudinal velocity profile.

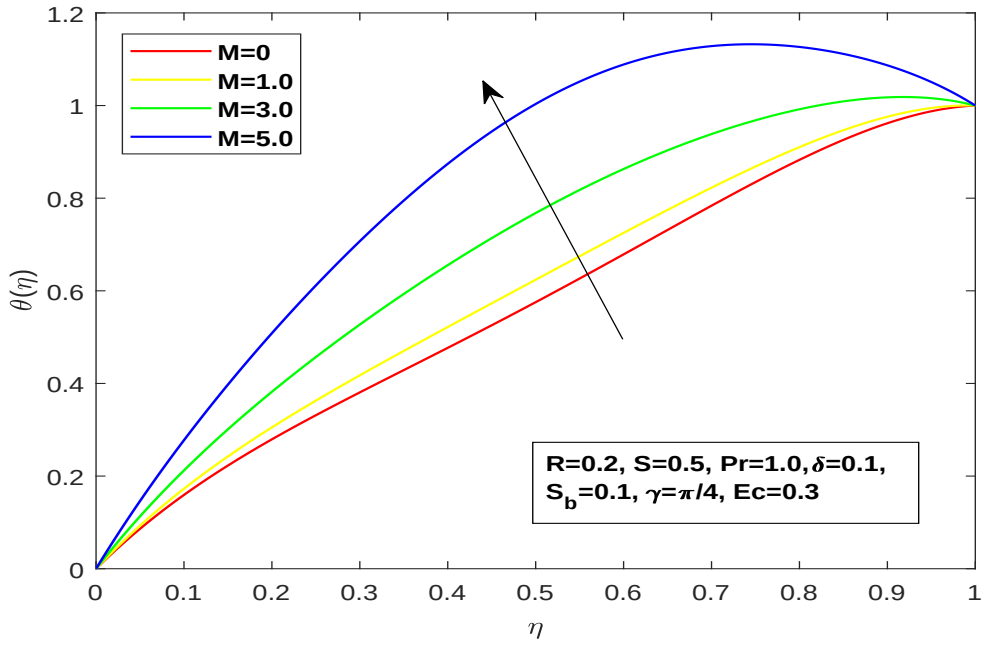

FIGURE 3.5: Impact of the magnetic parameter M on the temperature profile.

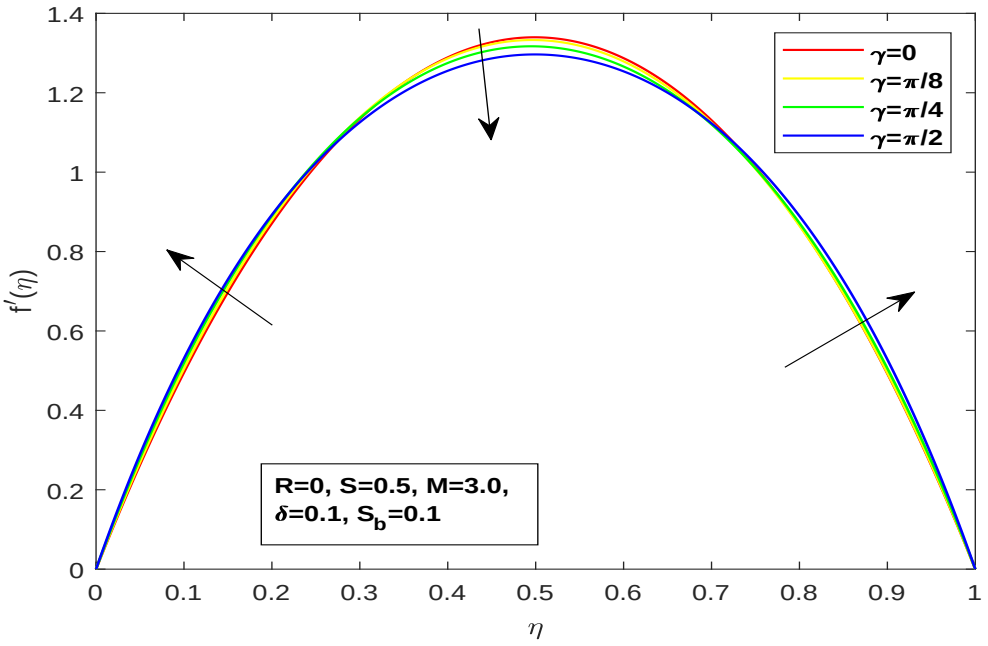

FIGURE 3.6: Impact of the magnetic inclination angle γ on the longitudinal velocity profile.

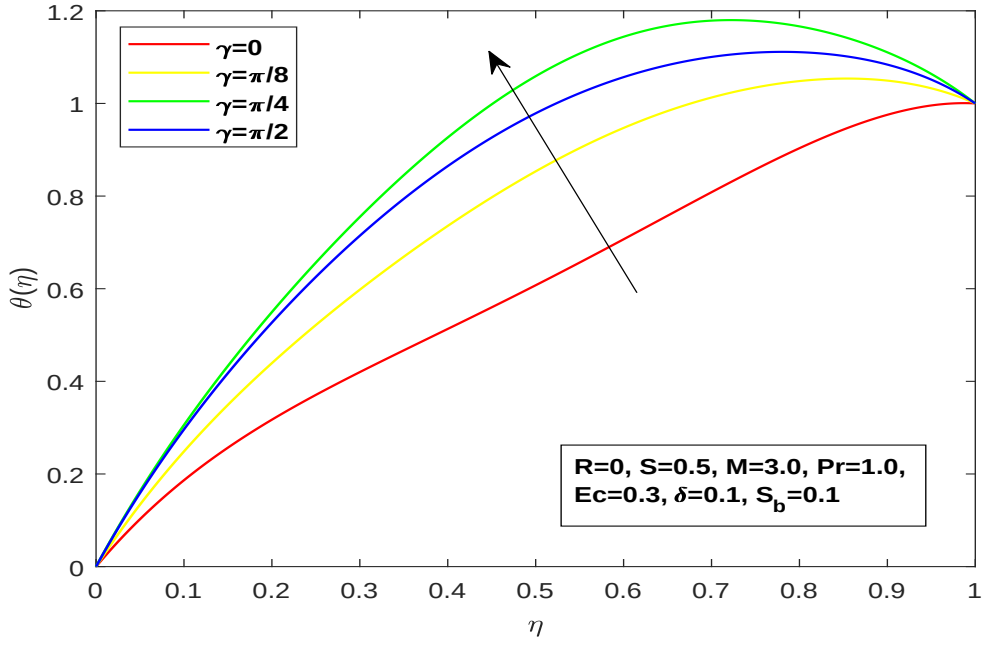

FIGURE 3.7: Imapct of the magnetic inclination angle γ on the temperature profile.

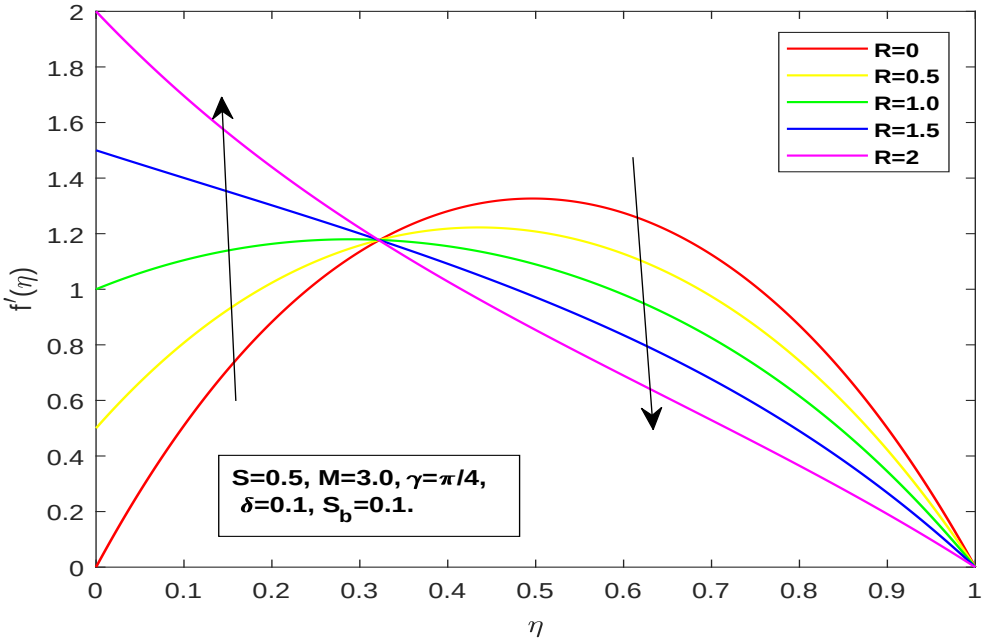

FIGURE 3.8: Impact of the lower plate stretching parameter R on the longitudinal velocity profile.

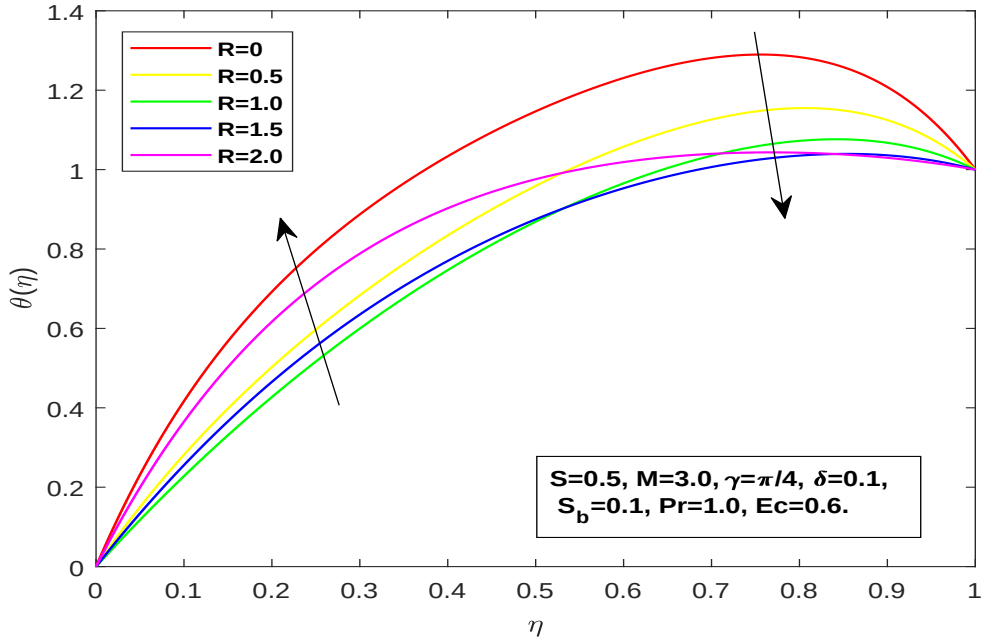

FIGURE 3.9: Impact of the lower plate stretching parameter R on the temperature profile.

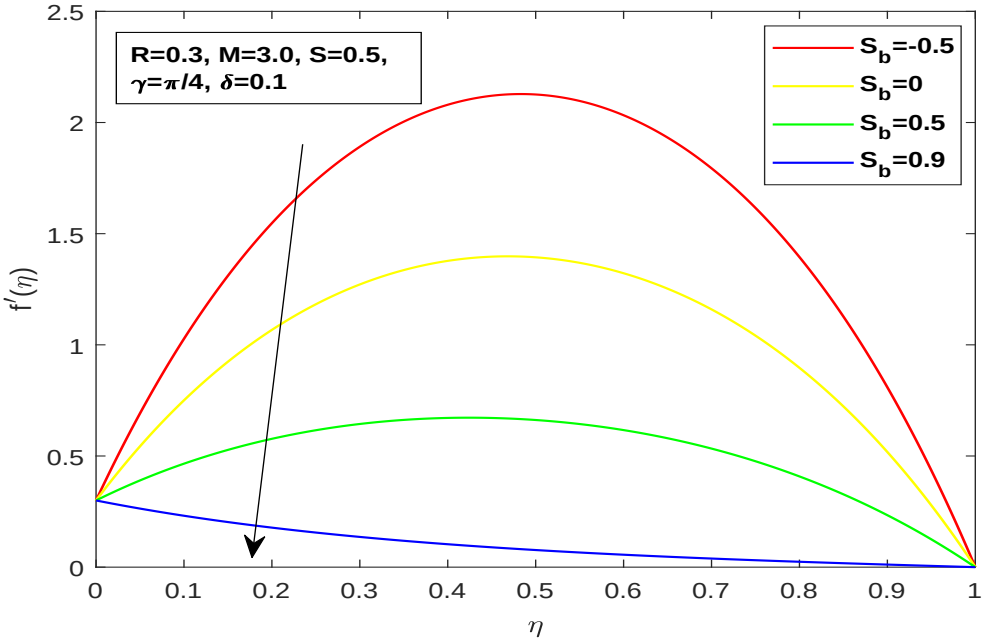

FIGURE 3.10: Impact of the lower plate suction/injection parameter S_b on the longitudinal velocity profile.

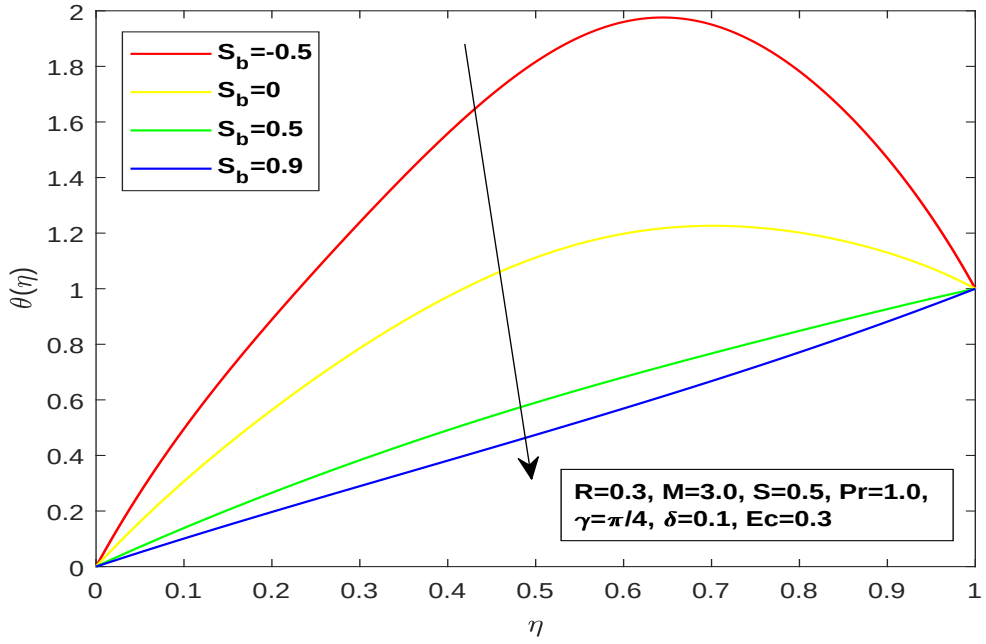

FIGURE 3.11: Impact of the lower plate suction/injection parameter S_b on the temperature profile.

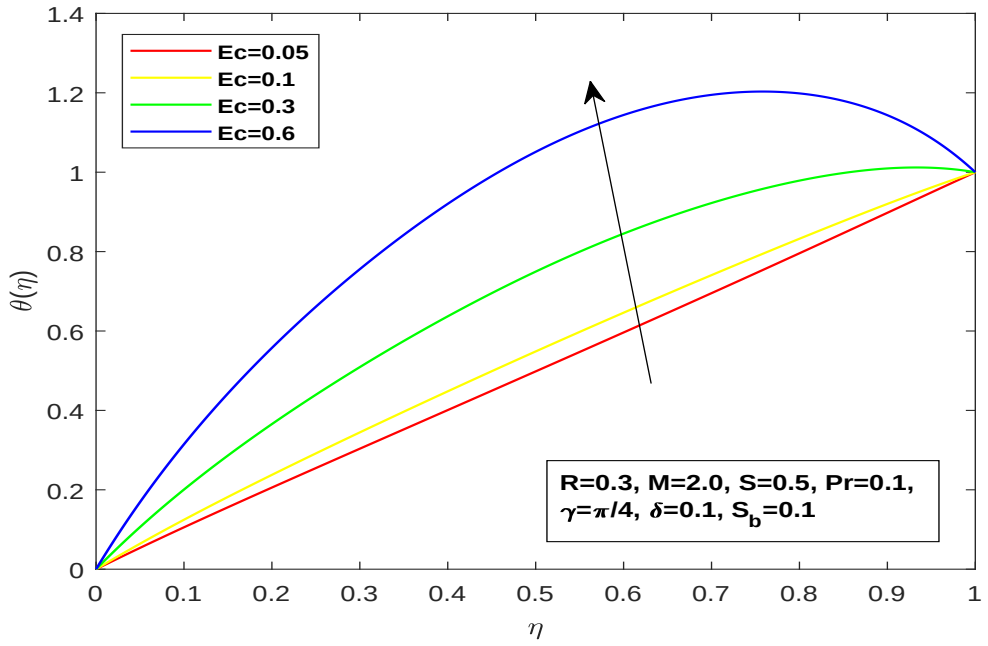

FIGURE 3.12: Impact of the Eckert E_c on the temperature profile.

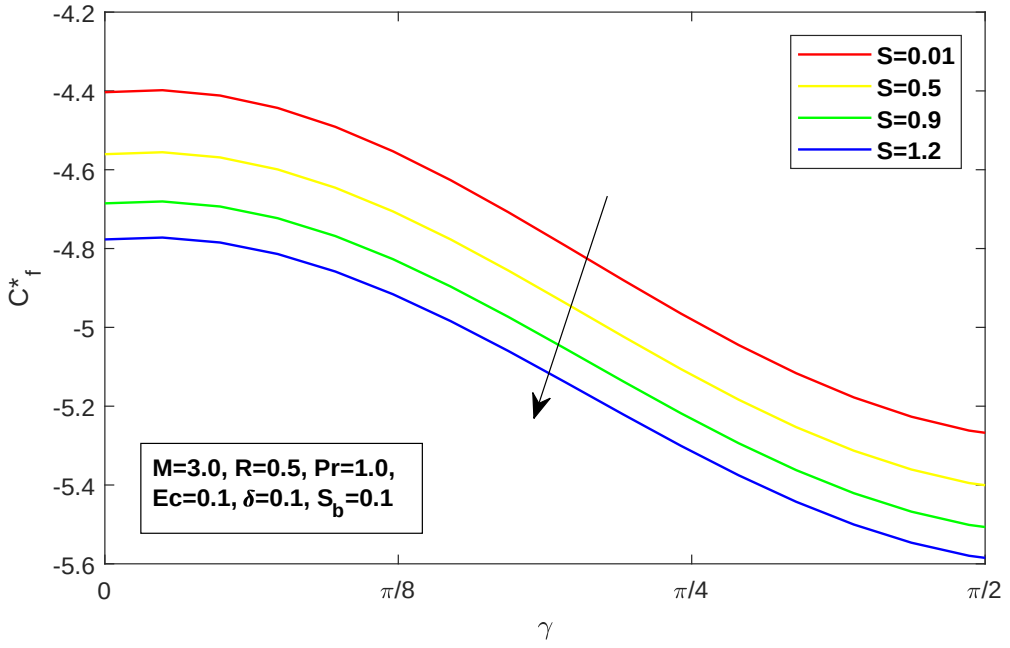

FIGURE 3.13: Impact of the magnetic inclination angle γ and the squeezing number S on the skin friction coefficient.

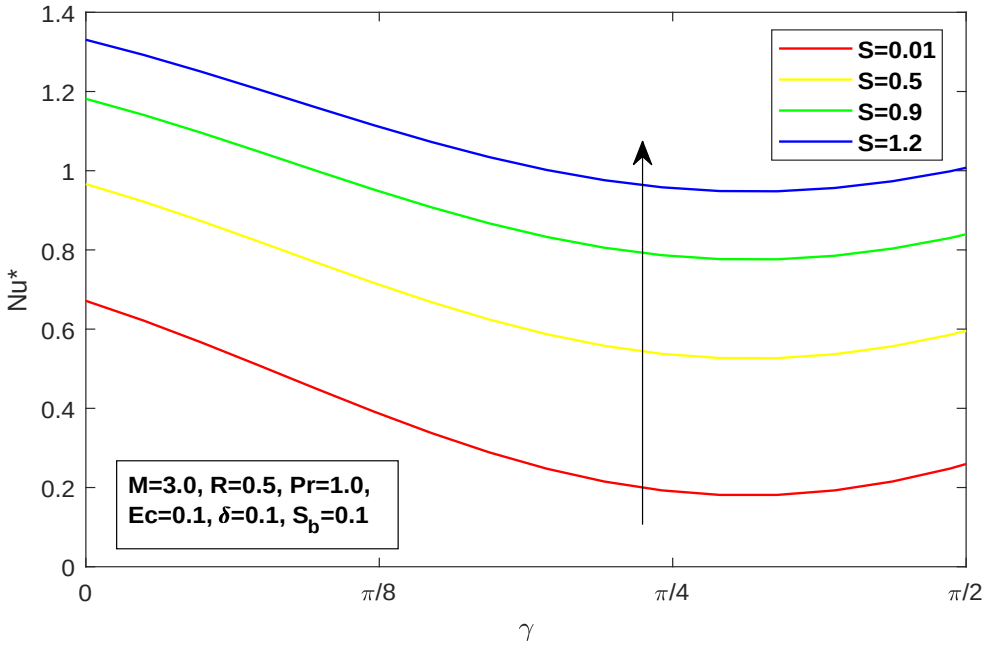

FIGURE 3.14: Impact of the magnetic inclination angle γ and the squeeze number S on the Nusselt number.

Chapter 4

Hybrid Nanofluid Flow between Parallel Plates

4.1 Introduction

This chapter extends the work of Su and Yin [30] by considering inclined magnetic field effects of unsteady squeezing hybrid nanofluid flow between parallel plates with suction/injection. The Alumina (Al_2O_3) and Copper (Cu) are considered as the hybrid nanoparticles and water is the base fluid. The necessary transformations are used to convert the governing coupled nonlinear PDEs into ODEs. In order to solve ODEs, the shooting method is implemented in MATLAB. At the end of this chapter, the numerical solution for various parameters for the dimensionless velocity and temperature is discussed. The generated numerical findings are examined using graphs.

4.2 Mathematical modeling

The problem considered in Chapter 3 is extended by using the hybrid nanofluid. Figure (3.1) shows the geometry of the problem. The flow is described in the

presence of suction/injection, viscous dissipation and Joule heating by continuity, momentum and energy equation are as follows:

$$\frac{\partial u}{\partial x}+\frac{\partial v}{\partial y}=0. \tag{4.1}$$

$$\frac{\partial u}{\partial t}+u\frac{\partial u}{\partial x}+v\frac{\partial u}{\partial y}=\frac{-1}{\rho_{hnf}}\frac{\partial p}{\partial x}+\frac{\mu_{hnf}}{\rho_{hnf}}\left(\frac{\partial^2 u}{\partial x^2}+\frac{\partial^2 u}{\partial y^2}\right)+ \frac{\sigma_{hnf}B_m^2}{\rho_{hnf}}\sin\gamma\left(v\cos\gamma-u\sin\gamma\right). \tag{4.2}$$

$$\frac{\partial v}{\partial t}+u\frac{\partial v}{\partial x}+v\frac{\partial v}{\partial y}=\frac{-1}{\rho_{hnf}}\frac{\partial p}{\partial y}+\frac{\mu_{hnf}}{\rho_{hnf}}\left(\frac{\partial^2 v}{\partial x^2}+\frac{\partial^2 v}{\partial y^2}\right)+ \frac{\sigma_{hnf}B_m^2}{\rho_{hnf}}\sin\gamma\left(u\sin\gamma-v\cos\gamma\right). \tag{4.3}$$

$$\frac{\partial T}{\partial t}+u\frac{\partial T}{\partial x}+v\frac{\partial T}{\partial y}=\frac{\kappa_{hnf}}{\rho C_{p\ hnf}}\left(\frac{\partial^2 T}{\partial x^2}+\frac{\partial^2 T}{\partial y^2}\right)+\frac{\mu_{hnf}}{\rho C_{p\ hnf}}\left[2\left(\frac{\partial u}{\partial x}\right)^2+ 2\left(\frac{\partial v}{\partial y}\right)^2+\left(\frac{\partial u}{\partial y}+\frac{\partial v}{\partial x}\right)^2\right]+\frac{\sigma_{hnf}B_m^2}{\rho C_{p\ hnf}}\left(u\sin\gamma-v\cos\gamma\right)^2. \tag{4.4}$$

The corresponding boundary conditions of lower and upper plates are:

$$\left.\begin{aligned} &At\ \ y=0,\\ &u=u_s=\frac{bx}{1-\alpha t},\quad v=v_c=-\frac{v_0}{(1-\alpha t)^{\frac{1}{2}}},\\ &T=T_0.\\ &At\ \ y=H(t),\\ &u=0,\qquad\qquad u=u_s=\frac{bx}{1-\alpha t},\\ &v=v_H=\frac{dH}{dt}=-\frac{\alpha l}{2(1-\alpha t)^{\frac{1}{2}}},\\ &T=T_H=T_0+\left(\frac{T_0}{1-\alpha t}\right). \end{aligned}\right\} \tag{4.5}$$

Here, u_s denotes lower plate stretching velocity, v_c represents lower plate mass flux velocity, v_H denotes upper plate velocity, T_0 is the lower plate surface temperature and T_H denotes the upper plate surface temperature. The following similarity transformations are used to convert partial differential equations into set of ordinary differential equations.

$$\left.\begin{aligned} u &= \tfrac{-x}{H(t)} v_H f'(\eta), \\ v &= v_H f(\eta), \\ \theta(\eta) &= \frac{T - T_0}{T_H - T_0}, \\ \eta &= \tfrac{y}{H(t)}, \\ H(t) &= l(1 - \alpha t)^{\frac{1}{2}}. \end{aligned}\right\} \tag{4.6}$$

4.3 Dimensionless Structure of the Governing Equation

Since the continuity equation (4.1) has been verified in Chapter 3.
By following the same steps as before, the momentum equations (4.2) and (4.3) as well as the energy equation (4.4) have the following dimensionless form.

$$\begin{aligned} &f^{(iv)} - A_1 A_2 S \left(\eta f''' + 3f'' + f' f'' - f f'''\right) - A_1 A_3 M^2 \\ &\sin\gamma \left(\sin\gamma f'' + 2\delta \cos\gamma f'\right) = 0, \end{aligned} \tag{4.7}$$

$$\begin{aligned} &\theta'' + \left(\frac{A_5}{A_4}\right) P_r S \left(f\theta' - \eta\theta' - 2\theta\right) + E_c P_r \left[\left(\frac{1}{A_1 A_4}\right)\left(f''^2 + 4\delta^2 f'^2\right)\right. \\ &\left. + \left(\frac{A_3}{A_4}\right) M^2 \left(f'^2 \sin^2\gamma + \delta^2 f^2 \cos^2\gamma + 2\delta f f' \sin\gamma\cos\gamma\right)\right] = 0, \end{aligned} \tag{4.8}$$

subject to boundary conditions:

$$\left.\begin{aligned} f(0) = S_b, \quad f'(0) = R, \quad \theta(0) = 0, \\ f(1) = 1, \quad f'(1) = 0, \quad \theta(1) = 1, \end{aligned}\right\} \tag{4.9}$$

where S, Pr, M, E_c and R are the squeezing number, prandtl number, magnetic parameter, Eckert number and lower plate stretching parameter, respectively. The lower plate suction and injection is denoted by $S_b > 0$ and $S_b < 0$, respectively,

and $A_1 = \dfrac{\mu_f}{\mu_{hnf}}$, $A_2 = \dfrac{\rho_{hnf}}{\rho_f}$, $A_3 = \dfrac{\sigma_{hnf}}{\sigma_f}$, $A_4 = \dfrac{k_{hnf}}{k_f}$, $A_5 = \dfrac{(\rho C_p)_{hnf}}{(\rho C_p)_f}$.
Following correlation are used in the equation to obtain, [44]

$$A_1 = (1-\phi_1)^{2.5}(1-\phi_2)^{2.5},$$
$$A_2 = \left((1-\phi_2)\left\{(1-\phi_1) + \phi_1\frac{\rho_{n1}}{\rho_f}\right\} + \phi_2\frac{\rho_{n2}}{\rho_f}\right),$$
$$A_3 = \left(\frac{\sigma_{n2}(1+2\phi_2)+2\sigma_f\left\{\frac{\sigma_{n1}(1+2\phi_1)+2\sigma_f(1-\phi_1)}{\sigma_{n1}(1-\phi_1)+\sigma_f(2+\phi_1)}\right\}(1-\phi_2)}{\sigma_{n2}(1-\phi_2)+\sigma_f\left\{\frac{\sigma_{n1}(1+2\phi_1)+2\sigma_f(1-\phi_1)}{\sigma_{n1}(1-\phi_1)+\sigma_f(2+\phi_1)}\right\}(2+\phi_2)}\right)\left(\frac{\sigma_{n1}(1+2\phi_1)+2\sigma_f(1-\phi_1)}{\sigma_{n1}(1-\phi_1)+\sigma_f(2+\phi_1)}\right),$$
$$A_4 = \left[\left(\frac{\kappa_{n2}+2\kappa_{nf}-2\phi_2(\kappa_{nf}-\kappa_{n2})}{\kappa_{n2}+2\kappa_{nf}+\phi_2(\kappa_{nf}-\kappa_{n2})}\right)\left(\frac{(\kappa_{n1}+2\kappa_f)-2\phi_1(\kappa_f-\kappa_{n1})}{(\kappa_{n1}+2\kappa_f)+\phi_1(\kappa_f-\kappa_{n1})}\right)\right],$$
$$A_5 = \left[(1-\phi_2)\left\{(1-\phi_1) + \phi_1\frac{(\rho C_p)_{n1}}{(\rho C_p)_f}\right\} + \phi_2\frac{(\rho C_p)_{n2}}{(\rho C_p)_f}\right].$$

TABLE 4.1: Thermophysical properties of hybrid nanofluid

Thermophysical Properties	**Hybrid Nanofluid**
Density	$\rho_{hnf} = (1-\phi_2)\left[(1-\phi_1)\rho_f + \phi_1\rho_{n1}\right] + \phi_2\rho_{n2}$
Heat capacity	$(\rho C_p)_{hnf} = (1-\phi_2)$ $\left[(1-\phi_1)(\rho C_p)_f + \phi_1(\rho C_p)_{n1}\right] + \phi_2(\rho C_p)_{n2}$
Dynamic viscosity	$\mu_{hnf} = \frac{\mu_f}{(1-\phi_1)^{2.5}(1-\phi_2)^{2.5}}$
Thermal conductivity	$\kappa_{hnf} = \frac{\kappa_{n2}+2\kappa_{nf}-2\phi_2(\kappa_{nf}-\kappa_{n2})}{\kappa_{n2}+2\kappa_{nf}+\phi_2(\kappa_{nf}-\kappa_{n2})} \times (\kappa_{nf})$ where, $\kappa_{nf} = \frac{\kappa_{n1}+2\kappa_f-2\phi_1(\kappa_f-\kappa_{n1})}{\kappa_{n1}+2\kappa_f+\phi_1(\kappa_f-\kappa_{n1})} \times (\kappa_f)$
Electrical conductivity	$\sigma_{hnf} = \frac{\sigma_{n2}+2\sigma_{nf}-2\phi_2(\sigma_{nf}-\sigma_{n2})}{\sigma_{n2}+2\sigma_{nf}+\phi_2(\sigma_{nf}-\sigma_{n2})} \times (\sigma_{nf})$ where, $\sigma_{nf} = 1 + \frac{3\left(\frac{\sigma_{n1}}{\sigma_f}-1\right)\phi_1}{2+\frac{\sigma_{n1}}{\sigma_f}-\left(\frac{\sigma_{n1}}{\sigma_f}-\right)\phi_1} \times (\sigma_f)$

TABLE 4.2: Thermophysical properties of Al_2O_3, Cu and water

Thermophysical Properties	Al_2O_3	**Cu**	**Water**
$\rho(kg/m^3)$	3970	8933	997.1
$C_p(J/kgK)$	765	385	4179
$\kappa(W/mK)$	40	400	0.613
$\sigma(S/m)$	3.69×10^7	5.96×10^7	0.05
Prandle number, Pr			6.2

4.4 Numerical Treatment

This section is dedicated to the implementation of the shooting method to solve the transformed ODEs (4.7) and (4.8) subject to the boundary conditions (4.9). One can easily observe that (4.7) is independent of θ, so we will first find the solution for (4.7). For this purpose, the following notations are used:

$$\begin{aligned} f &= g_1, \\ f' &= g_1' = g_2, \\ f'' &= g_2' = g_3, \\ f''' &= g_3' = g_4, \\ f^{(iv)} &= g_4'. \end{aligned}$$

Utilizing the above notations, we have the following system of four first order differential equations is obtained,

$$\left.\begin{aligned} g_1' &= g_2; & g_1(0) &= S_b = \frac{2v_0}{\alpha l}, \\ g_2' &= g_3; & g_2(0) &= R = \frac{u_\circ \delta}{v_H}, \\ g_3' &= g_4; & g_3(0) &= \alpha_1, \\ g_4' &= A_1 A_2 S(3g_3 + \eta g_4 + g_2 g_3 - g_1 g_4) + \\ & A_1 A_3 M^2 \sin\gamma(2\delta\cos\gamma g_2 + \sin\gamma g_2); & g_4(0) &= \alpha_2. \end{aligned}\right\} \tag{4.10}$$

To solve the above system by using Runge Kutta method of order four, two missing initial conditions are assumed to be α_1 and α_2, such that:

$$\begin{aligned} g_1(\eta, \alpha_1, \alpha_2)_{\eta=1} - 1 &= 0, \\ g_2(\eta, \alpha_1, \alpha_2)_{\eta=1} - 0 &= 0. \end{aligned}$$

These non-linear algebraic equations are solved for α_1 and α_2 by Newton's method which has the following iterative scheme:

$$\begin{bmatrix} u^{n+1} \\ v^{n+1} \end{bmatrix} = \begin{bmatrix} u^{n} \\ v^{n} \end{bmatrix} - \begin{bmatrix} \frac{\partial g_1}{\partial \alpha_1} & \frac{\partial g_1}{\partial \alpha_2} \\ \frac{\partial g_2}{\partial \alpha_1} & \frac{\partial g_2}{\partial \alpha_2} \end{bmatrix}^{-1} \begin{bmatrix} g_1(\alpha_1, \alpha_2) - 1 \\ g_2(\alpha_1, \alpha_2) - 0 \end{bmatrix}. \tag{4.11}$$

To incorporate the above formula, we further need the following derivatives:

$$\begin{aligned} &\frac{\partial g_1}{\partial \alpha_1} = g_5, \quad \frac{\partial g_2}{\partial \alpha_1} = g_6, \quad \frac{\partial g_3}{\partial \alpha_1} = g_7, \quad \frac{\partial g_4}{\partial \alpha_1} = g_8, \\ &\frac{\partial g_1}{\partial \alpha_2} = g_9, \quad \frac{\partial g_2}{\partial \alpha_2} = g_{10}, \quad \frac{\partial g_3}{\partial \alpha_2} = g_{11}, \quad \frac{\partial g_4}{\partial \alpha_2} = g_{12}. \end{aligned}$$

As the result of these notations, the Newton's iterative scheme gets the form:

$$\begin{bmatrix} u^{n+1} \\ v^{n+1} \end{bmatrix} = \begin{bmatrix} u^{n} \\ v^{n} \end{bmatrix} - \begin{bmatrix} g_5 & g_9 \\ g_6 & g_{10} \end{bmatrix}^{-1} \begin{bmatrix} g_1(\alpha_1, \alpha_2) - 1 \\ g_2(\alpha_1, \alpha_2) - 0 \end{bmatrix}. \tag{4.12}$$

In order to achieve the numerical solution, we further differentiate the ordinary differential equation (4.2) w.r.to α_1 and α_2. Hence, the following system of twelve first order coupled differential equation is achieved with initial values.

$$\begin{aligned}
&g_1' = g_2; && g_1(0) = S_b = \frac{2v_0}{\alpha l}, \\
&g_2' = g_3; && g_2(0) = R = \frac{u_s \delta}{v_H}, \\
&g_3' = g_4; && g_3(0) = \alpha_1, \\
&g_4' = A_1 A_2 S(3g_3 + \eta g_4 + g_2 g_3 - g_1 g_4) \\
&\quad + A_1 A_3 M^2 \sin\gamma(2\delta \cos\gamma g_2 + \sin\gamma g_2); && g_4(0) = \alpha_2, \\
&g_5' = g_6; && g_5(0) = 0, \\
&g_6' = g_7; && g_6(0) = 0, \\
&g_7' = g_8; && g_7(0) = 1, \\
&g_8' = A_1 A_2 S(3g_7 + \eta g_8 + g_6 g_3 - g_5 g_4 + g_2 g_7 - g_1 g_8) \\
&\quad + A_1 A_3 M^2 \sin\gamma(2\delta \cos\gamma g_6 + \sin\gamma g_7); && g_8(0) = 0, \\
&g_9' = g_{10}; && g_9(0) = 0, \\
&g_{10}' = g_{11}; && g_{10}(0) = 0,
\end{aligned}$$

$$
\begin{aligned}
&g_{11}' = g_{12}; && g_{11}(0) = 0,\\
&g_{12}' = A_1A_2S(3g_{11} + \eta g_{12} + g_{10}g_3 - g_9g_4 + g_2g_{11} - g_1g_{12})\\
&+ A_1A_3M^2 \sin\gamma(2\delta\cos\gamma g_{10} + \sin\gamma g_{11}); && g_{12}(0) = 1.
\end{aligned}
$$

The Runge Kutta method of order four is used to solve the above initial value problem, where α_1 and α_2 are unknown initial conditions. The iterative process is repeated until the criteria listed below is met:

$$\max\left[\mid g_1(\eta, \alpha_1, \alpha_2) - 1 \mid, \mid g_2(\eta, \alpha_1, \alpha_2) \mid\right] < \epsilon,$$

for an arbitrarily small positive value of ϵ. Throughout this chapter ϵ has been taken as $(10)^{-6}$.

Since (4.9) and (4.10) are coupled equations. So (4.10) will be solved separately by incorporating the solution of (4.9). For this purpose let us denote:

$$\theta = Y_1, \qquad \theta' = Y_1' = Y_2, \qquad \theta'' = Y_2',$$

to get the following first order ODEs.

$$
\left.
\begin{aligned}
&Y_1' = Y_2; && Y_1(0) = 0,\\
&Y_2' = -\left[\left(\frac{A_5}{A_4}\right) P_rS\left(fY_2 - \eta Y_2 - 2Y_1\right) +\right.\\
&\left(\frac{1}{A_1A_4}\right) P_rE_c\left\{f''^2 + 4\delta^2 f'^2 + \left(\frac{A_3}{A_4}\right) M^2\left(f'^2\sin^2\gamma\right.\right.\\
&\left.\left.+ f^2\delta^2\cos^2\gamma + 2\delta f f'\cos\gamma\sin\gamma\right)\right\}\Big]; && Y_2(0) = m.
\end{aligned}
\right\} \tag{4.13}
$$

The above IVP is solved numerically by Runge Kutta method of order four. In the above initial value problem, the missing condition m is to be chosen such that:

$$Y_1(\eta, m)_{\eta=1} - 1 = 0, \tag{4.14}$$

To solve the above algebraic equation (4.16) the Newton's method is used which has the following iterative scheme:

$$m^{n+1} = m^n - \left(\frac{\partial Y_1}{\partial m}\right)^{-1} (Y_1(\eta, m^n)_{\eta=1} - 1)\,.$$

Further considering the following derivatives:

$$\frac{\partial Y_1}{\partial m} = Y_3, \qquad \frac{\partial Y_2}{\partial m} = Y_4.$$

to formulate the following Newton's iterative scheme:

$$m^{n+1} = m^n - [Y_3(\eta, m^n)_{\eta=1}]^{-1} (Y_1(\eta, m^n)_{\eta=1} - 1)\,. \tag{4.15}$$

Here n is the number of iterations ($n = 0, 1, 2, 3, 4, 5, ...$).
To incorporate the new derivative Y_3 and Y_4 system (4.13) is further differentiated w.r.to m, to get the following IVP:

$$\begin{aligned}
&Y_1' = Y_2; && Y_1(0) = 0,\\
&Y_2' = -\left[\left(\frac{A_5}{A_4}\right) P_r S\,(D_1 Y_2 - \eta Y_2 - 2Y_1) + \left(\frac{1}{A_1 A_4}\right) P_r E_c \left\{D_3^2 + 4\delta^2\right.\right.\\
&\left.\left. D_2^2 + \frac{A_3}{A_4} M^2 \left(D^2 - 2\sin^2\gamma + D_1^2\delta^2\cos^2\gamma + 2\delta D_1 D_2 \cos\gamma \sin\gamma\right)\right\}\right]; && Y_2(0) = m,\\
&Y_3' = Y_4; && Y_3(0) = 0,\\
&Y_4' = -\left(\frac{A_5}{A_4}\right) P_r S\,(D_1 Y_4 - \eta Y_4 - 2Y_3)\,; && Y_1(0) = 1.
\end{aligned}$$

The Runge Kutta method of order four has been used to solve the IVP consisting of the above four ODE's for some suitable choices of m. The missing condition m is updated by using Newton's scheme (4.15). If the following criterion is fulfilled the iterative process is stopped:

$$|Y_1(\eta, m) - 1| < \epsilon,$$

for an arbitrarily small positive value of ϵ. Here ϵ is taken as 10^{-10} throughout.

4.5 Results and Discussion

In this segment of thesis, the influence of various dimensionless parameters on velocity and temperature profile for the hybrid nanofluid flow have been discussed and presented through the figures 4.1-4.13. The thermophysical properties of $Cu - Al_2O_3$/water are used. The dimensionless parameters that influenced the velocity and temperature profile are squeezing number (S), magnetic parameter (M) , lower plates stretching parameter (R), magnetic inclination angle (γ), Eckert number (Ec), hybrid nanoparticles volume fractions (ϕ_1 and ϕ_2) and lower plate suction/injection parameter (S_b). The value of ϕ_1 and ϕ_2 have been taken from [44].

Figure 4.1 demonstrates the distribution of fluid velocity close to the lower or upper end of plates are decreasing due to rising of the squeeze number, but for the velocity an opposite effect has been observed close to the centre between the plates. It is noted from Figure 4.2 that rising the values of the squeezing parameter causes reduction in the temperature. When the plates move close to each other, the temperature field will be comparatively high.

Figure 4.3 and 4.4 represent the velocity and temperature profile for the variation of magnetic parameter. It has been observed in Figure 4.3 that an increase in the magnetic parameter causes the fluid velocity to increase at both ends (lower and upper) of the plates, but the fluid velocity near the centre, quite slightly, shows a noticeable decrease. The fluid in the central regions has larger Lorentz force than the fluid near the plates. The reason is that the Lorentz force in fluid motion presents resistance, so it makes velocity slow down close the central region of plates. Figure 4.4 shows that the fluid temperature rises from the lower to upper plate surface when the magnetic field parameter rises. For the larger magnetic value, the fluid temperature increases not only near the upper surface but also in the centre between the plates. Actually, the strong magnetic field affects the temperature distribution in the regions. Large friction along with a strong magnetic field generates more heat in fluids.

Velocity and temperature profile have been shown through Figures 4.5 and 4.6 by

rising value of the magnetic inclination angle. The angle of magnetic inclination ranges between 0 and $\pi/2$. Similar behaviors of velocity and temperature profile have been obtained from both figures when compared to the corresponding profiles of different magnetic parameter values. The angle of magnetic field inclination γ effects on both the fluid velocity and the temperature are similar to those of the magnetic parameter. Therefore, the transfer of fluid in the squeezing movement in practical applications related to momentum and heat control, the affects generated by changing the strength of the magnetic field can also be obtained by modifying the angle of magnetic field inclination.

Figure 4.7 and 4.8 show the affect of stretching parameter of the lower plate on the velocity and temperature profile. In Figure 4.7 the fluid velocity increases close to the lower plate as compared to the fluid velocity close to the upper plate. Furthermore, as the stretching parameter on the lower surface rises, the maximum value of velocity can be seen in the surface of lower plate. Figure 4.8 reflects that when we rise the stretching parameter of the lower plate, the fluid temperature above the lower plate decreases and increases thereafter, when we take the stretching parameter $R > 1.5$ the fluid temperature close to the lower plate increases.

Figure 4.9 and 4.10 represent the effects of lower plate suction/injection parameter on the fluid velocity and temperature profile. Figure 4.9 indicates that with increase in the lower plate injection/suction parameter, the velocity profile falls. The fluid having peak velocity does not occur in the central area when extending the lower plate for stronger suction through the lower plate and the velocity of the fluid monotonically decreases from the surface of the lower plate to the upper plate. Figure 4.10 shows that the temperature profile decrease as the injection/-suction parameter increases. It is found that the fluid having largest temperature appears at the central section within the two plates but not on the surface of upper plate when the injection/suction parameter S_b falls.

The temperature for different values of Eckert number was shown in Figure 4.11. A clear temperature rise is observed to increase the values of Eckert number. This increase in the thermal field is evident because Eckert has directly affects on the process of heat dissipation, which in turn increases the temperature field between

the plates. Figure 4.11 also indicates that the maximum fluid temperature occurs in the centre between the two plates for larger Eckert number, whereas it tends to be smaller in the upper plate.

Figure 4.12 and 4.13 demonstrate the effects of the squeeze parameter and magnetic angle on the coefficient of skin friction and the Nusselt number, where the magnetic inclination angle ranges among 0° to 90°. The absolute value of skin friction and Nusselt number may be noticed as a decreasing function of the angle of magnetic inclination. Whereas, for the increasing in squeeze parameter and keeping the angle of magnetic inclination fixed, the Nusselt number decreases and skin friction coefficient increases.

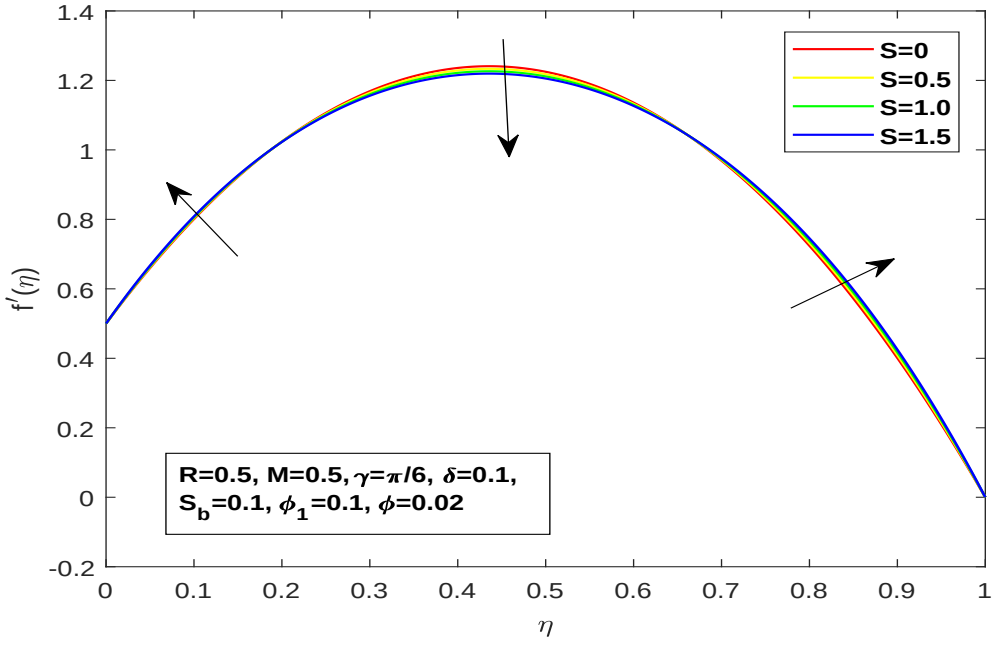

FIGURE 4.1: Impact of the squeeze number S on the longitudinal velocity profile.

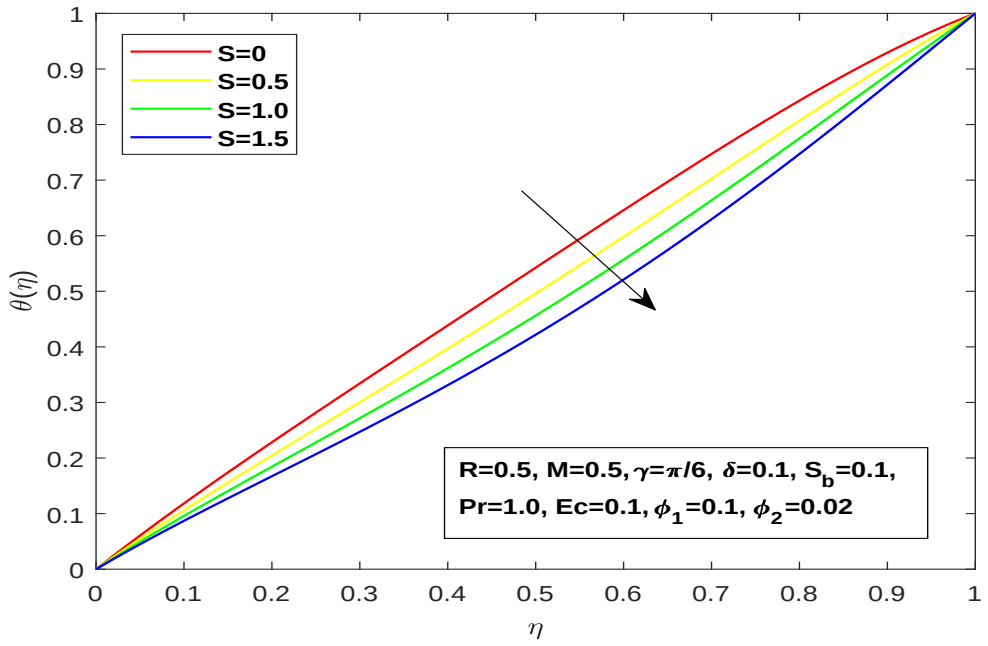

FIGURE 4.2: Impact of the squeeze number S on the temperature profile.

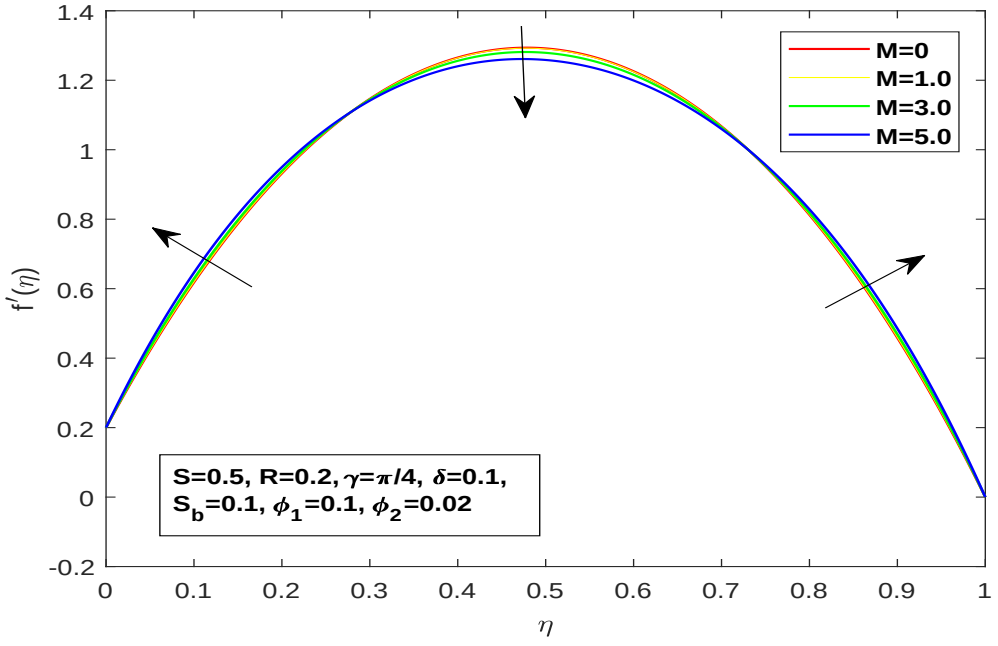

FIGURE 4.3: Impact of the magnetic parameter M on the longitudinal velocity profile.

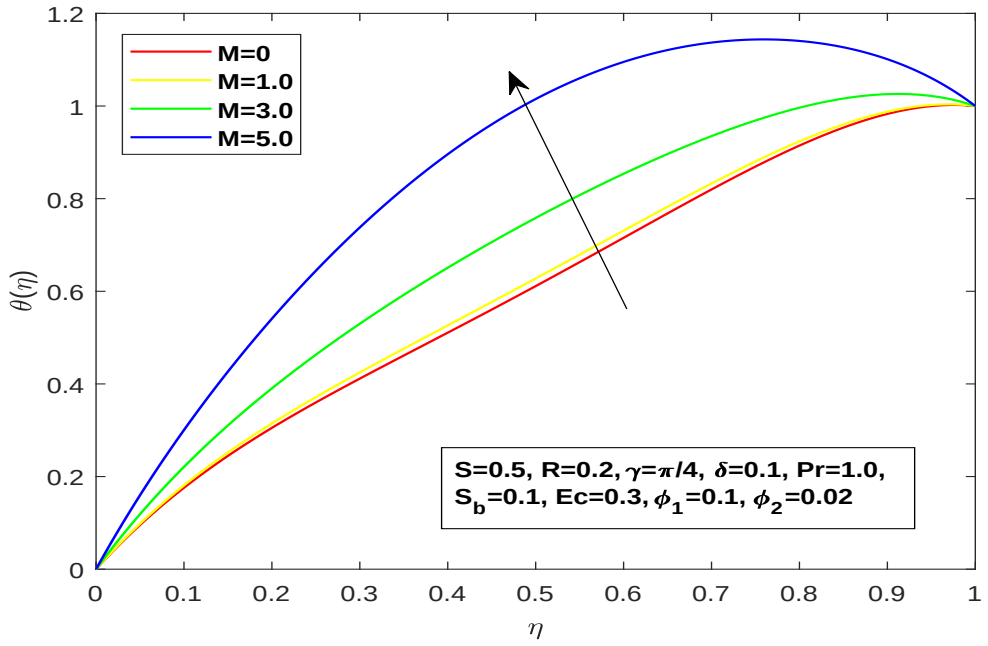

FIGURE 4.4: Impact of the magnetic parameter M on the temperature profile.

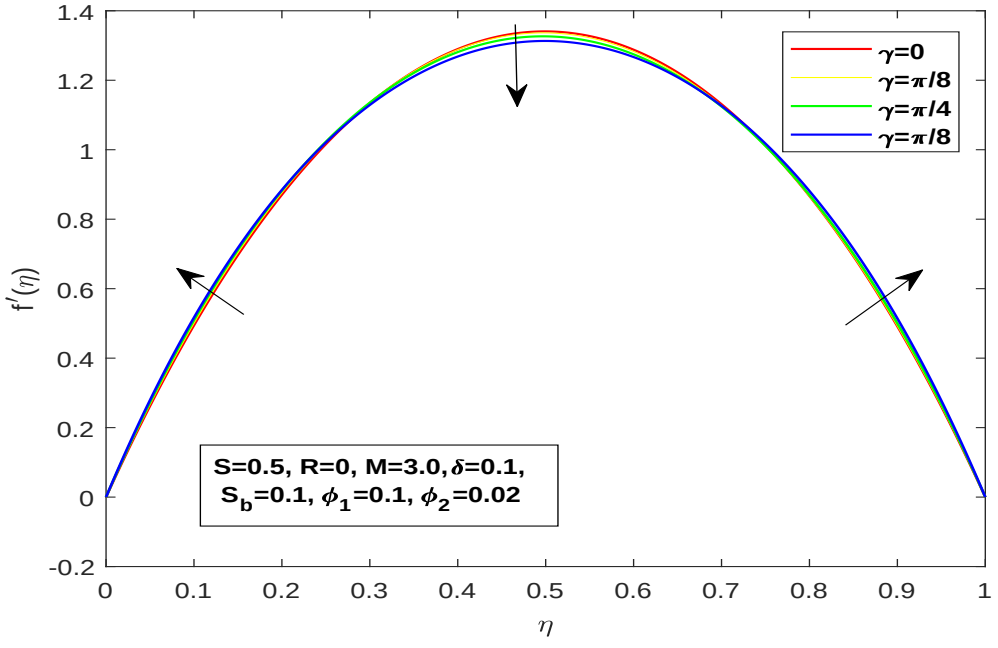

FIGURE 4.5: Impact of the magnetic inclination angle γ on the longitudinal velocity profile.

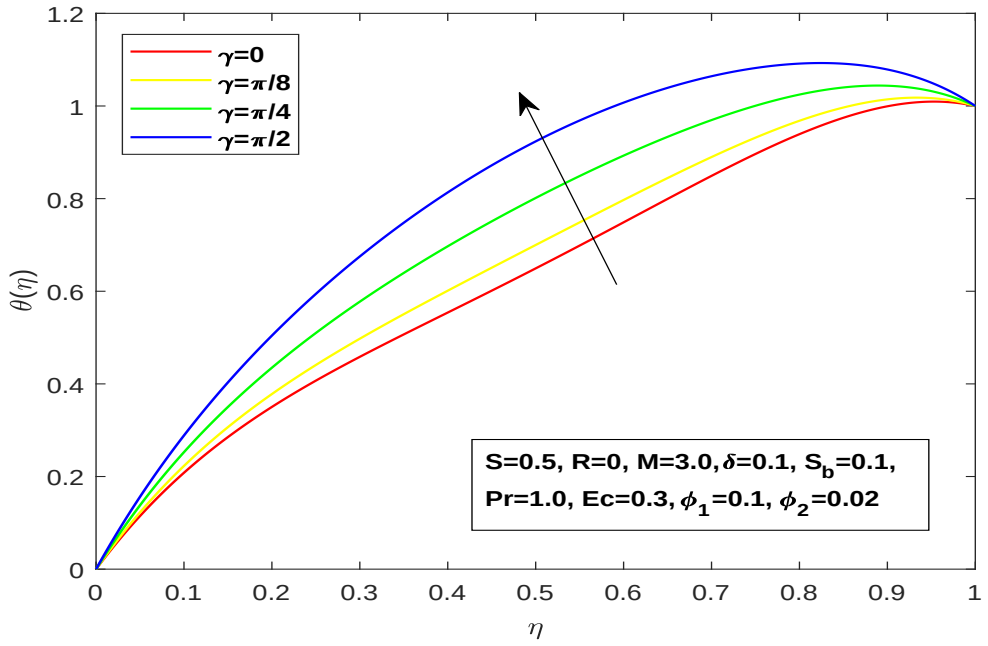

FIGURE 4.6: Impact of the magnetic inclination angle γ on the temperature profile.

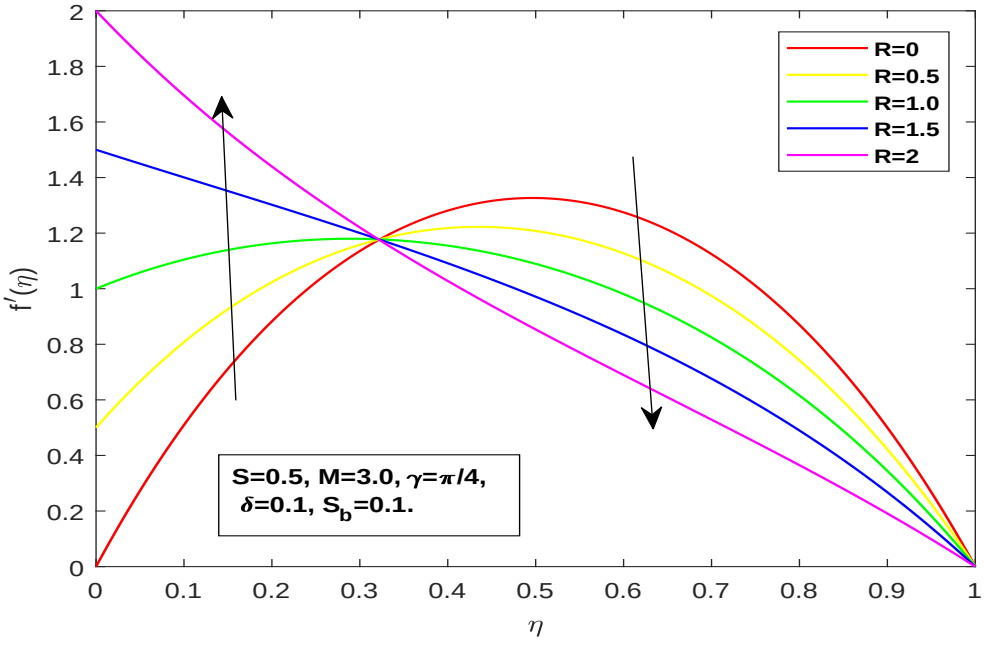

FIGURE 4.7: Impact of the lower plate stretching parameter R on the longitudinal velocity profile.

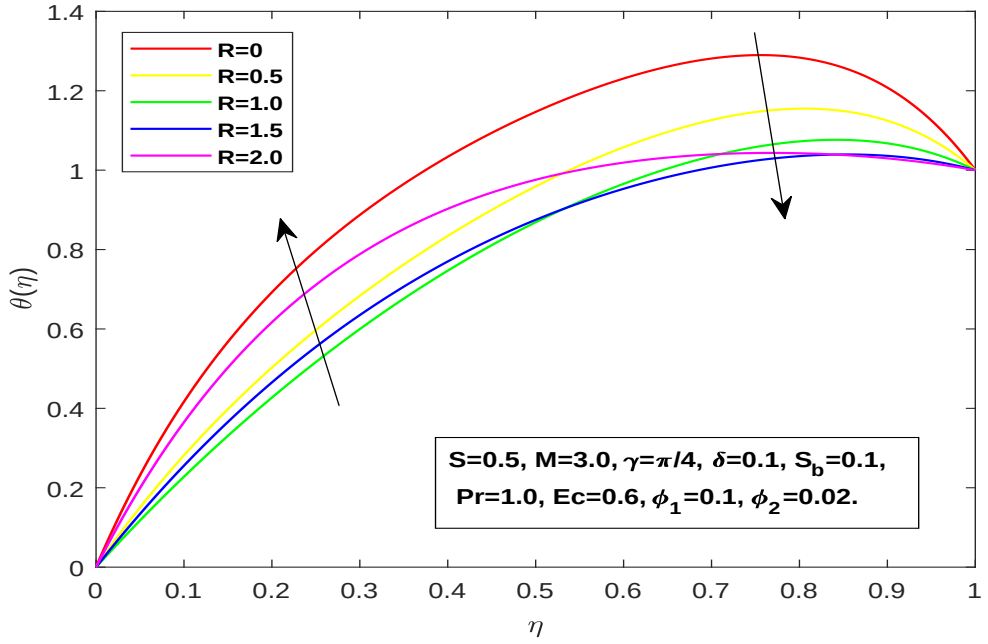

FIGURE 4.8: Impact of the lower plate stretching parameter R on the temperature profile.

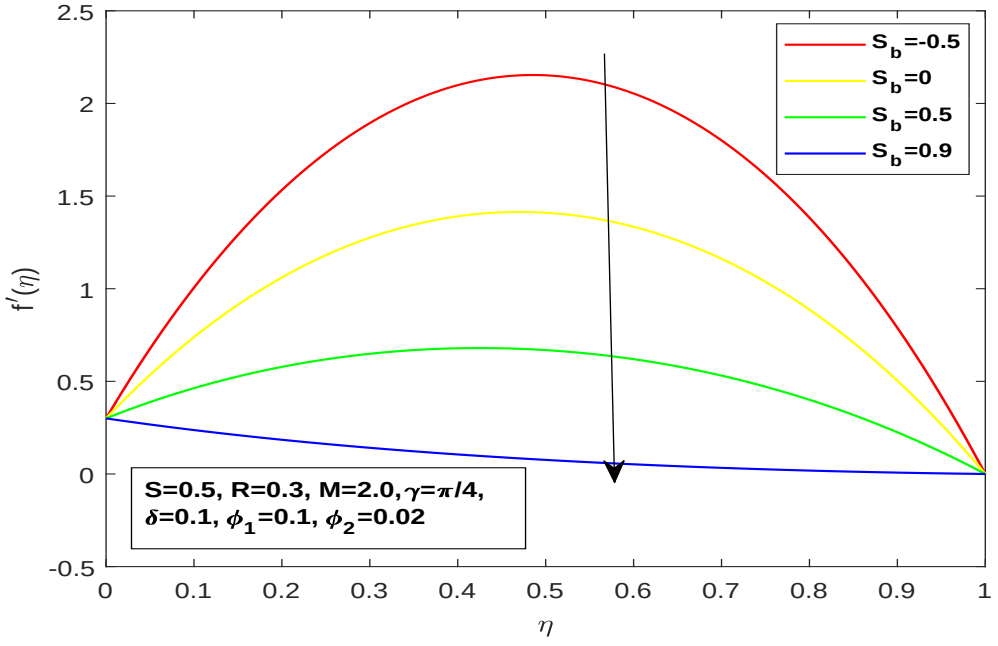

FIGURE 4.9: Impact of the lower plate suction/injection parameter S_b on the longitudinal velocity profile.

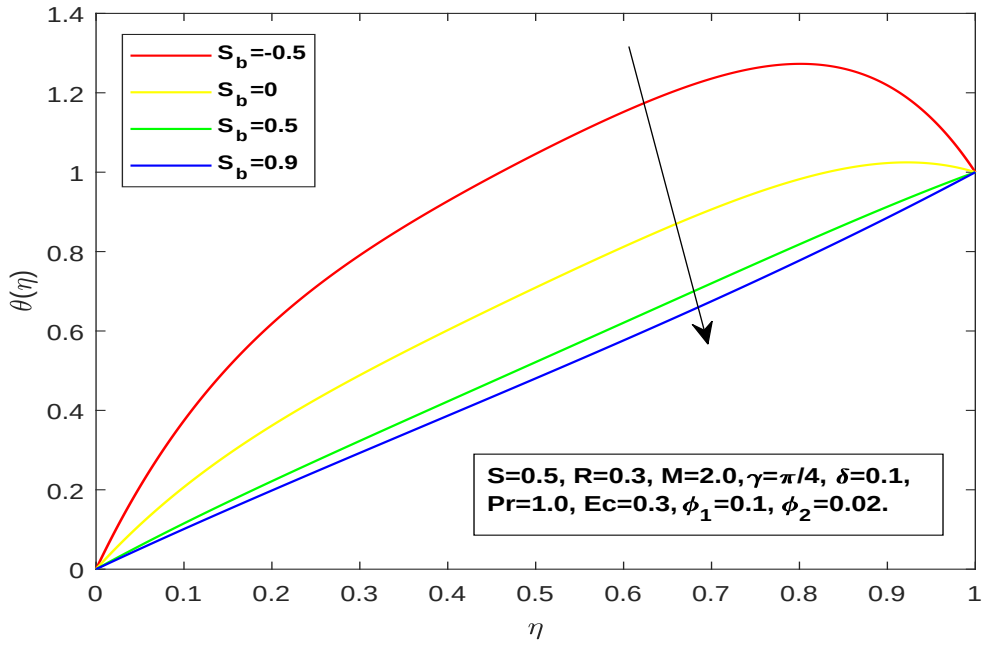

FIGURE 4.10: Impact of the lower plate suction/injection parameter S_b on the temperature profile.

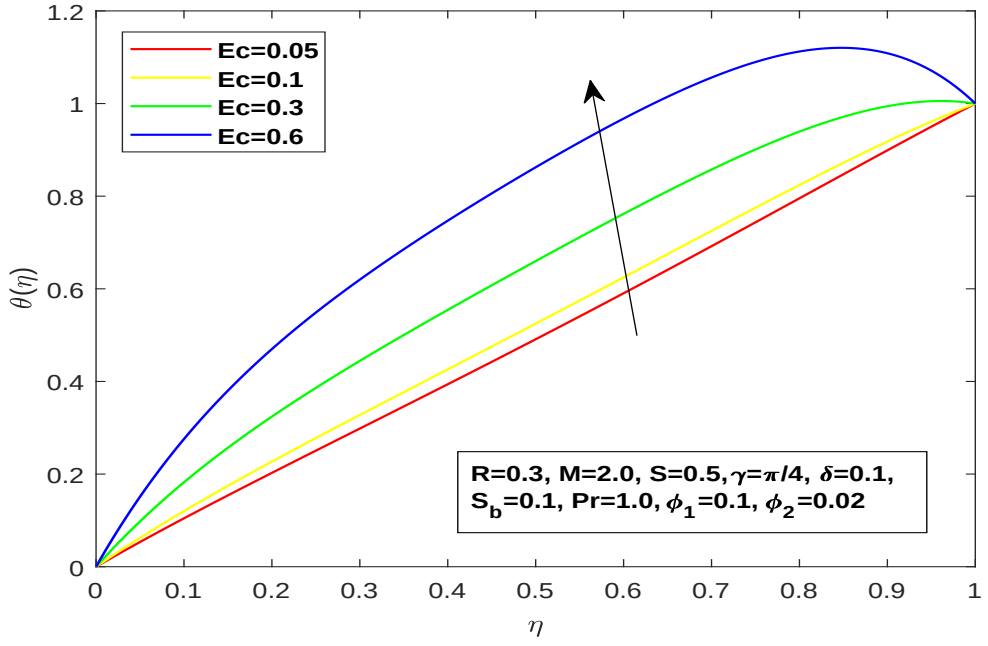

FIGURE 4.11: Impact of the Eckert Ec on the temperature profile.

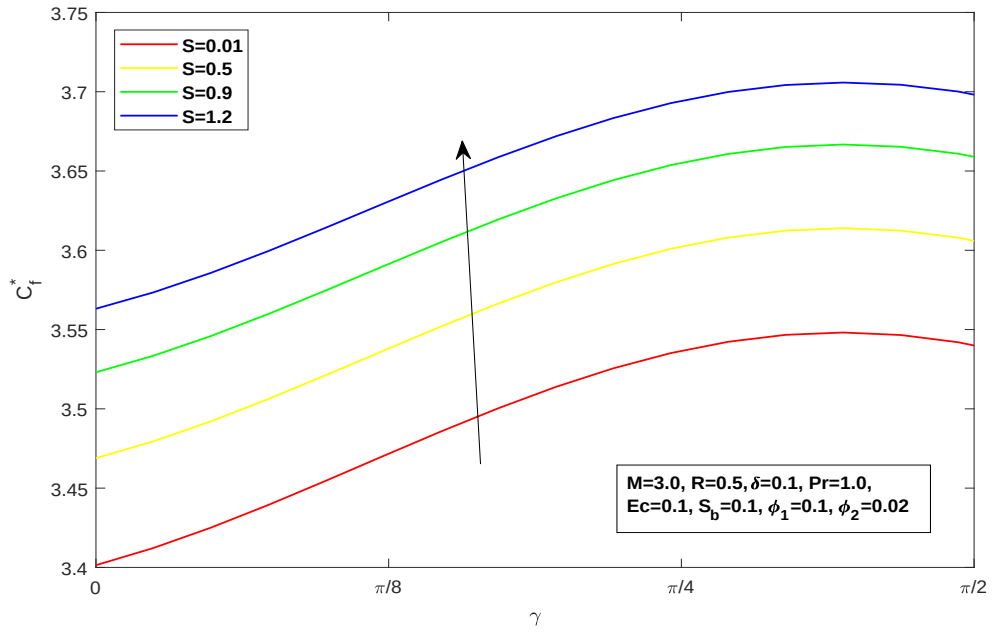

FIGURE 4.12: Impact of the magnetic inclination angle γ and the squeezing number S on the skin friction coefficient.

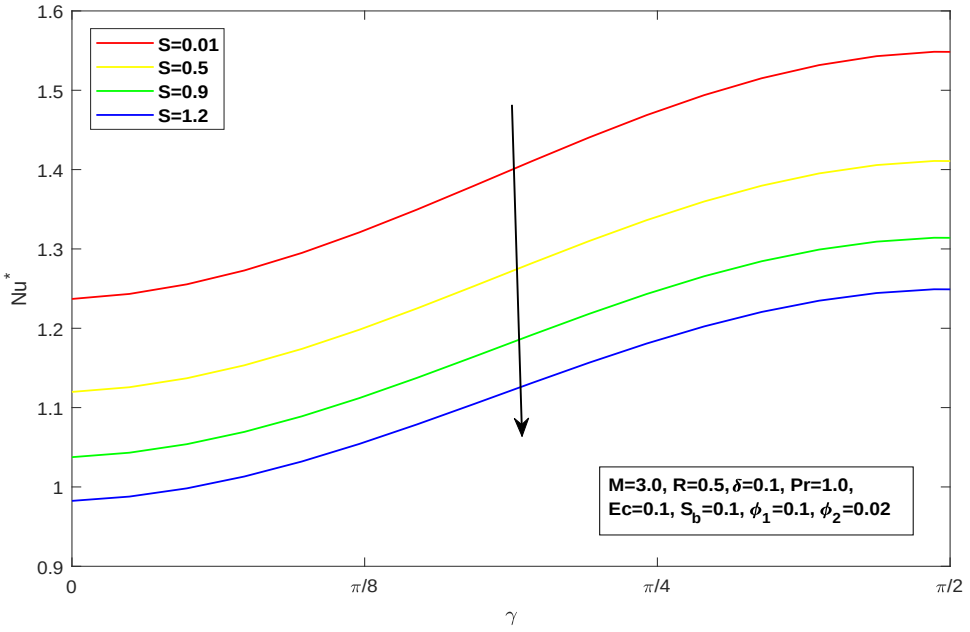

FIGURE 4.13: Impact of the magnetic inclination angle γ and the squeeze number S on the Nusselt number.

Chapter 5

Conclusion

This section will conclude the whole research eventually. Hence this section presents the precise analysis of an inclined magnetic field effects on the squeezed hybrid nanofluid flow between parallel plates with suction/injection through the stretching lower plate. By utilizing similarity transformation we reduced the set of nonlinear PDEs into a set of nonlinear ODEs and then solved numerically. Numerical results are obtained for the set of nonlinear ODEs by using the well known shooting technique with Runge Kutta method of order four (RK4). Significance of the effect of different physical parameters under discussion on the dimensionless velocity and temperature are describe graphically. The skin friction and the Nusselt number for different value of the distinctive governing parameters are also presented graphically. The following key notes are observed.

1. Increasing the value of squeeze parameter (S), the velocity close to the lower or upper end of plates is decreasing, but the velocity profile decreases at the centre of the plates and the temperature profile tends to decrease throughout.

2. The magnetic field (M) has a direct relation with the temperature profile and an inverse with the velocity profile.

3. Increasing the angle of magnetic inclination(γ), the velocity close to the lower or upper end of plates is decreasing, but an opposite effect has been

observed close to the centre between the plates. The temperature profile tends to increase.

4. The lower plate suction/injection parameter (S_b) is an inverse relation with the velocity and temperature profile.

5. Increasing the value of the Eckert number (Ec), the temperature profile tends to increase.

6. For the increment of squeeze parameter (S) and the angle of magnetic inclination (γ), the skin friction (C_f*) increases and the Nusselt number ($Nu*$) decreases. Moreover, both skin friction and Nusselt number are increasing function of angle of inclination.

Bibliography

[1] M. Stefan, "Experiment on apparent adhesion, academy of sciences in vienna. mathematical and natural sciences," 1874.

[2] X. Ran, Q. Zhu, and Y. Li, "An explicit series solution of the squeezing flow between two infinite plates by means of the homotopy analysis method," *Communications in Nonlinear Science and Numerical Simulation*, vol. 14, no. 1, pp. 119–132, 2009.

[3] M. Mustafa, T. Hayat, and S. Obaidat, "On heat and mass transfer in the unsteady squeezing flow between parallel plates," *Meccanica*, vol. 47, no. 7, pp. 1581–1589, 2012.

[4] U. Khan, N. Ahmed, M. Asadullah, and S. T. Mohyud-din, "Effects of viscous dissipation and slip velocity on two-dimensional and axisymmetric squeezing flow of cu-water and cu-kerosene nanofluids," *Propulsion and Power research*, vol. 4, no. 1, pp. 40–49, 2015.

[5] G. Domairry and A. Aziz, "Approximate analysis of mhd squeeze flow between two parallel disks with suction or injection by homotopy perturbation method," *Mathematical Problems in Engineering*, vol. 2009, 2009.

[6] T. Hayat and S. Hina, "Effects of heat and mass transfer on peristaltic flow of williamson fluid in a non-uniform channel with slip conditions," *International Journal for numerical methods in fluids*, vol. 67, no. 11, pp. 1590–1604, 2011.

[7] S. Ahmad, M. Farooq, M. Javed, and A. Anjum, "Slip analysis of squeezing flow using doubly stratified fluid," *Results in Physics*, vol. 9, pp. 527–533, 2018.

[8] ——, "Double stratification effects in chemically reactive squeezed sutterby fluid flow with thermal radiation and mixed convection," *Results in physics*, vol. 8, pp. 1250–1259, 2018.

[9] R. U. Haq, S. Nadeem, Z. H. Khan, and N. S. Akbar, "Thermal radiation and slip effects on mhd stagnation point flow of nanofluid over a stretching sheet," *Physica E: Low-dimensional systems and nanostructures*, vol. 65, pp. 17–23, 2015.

[10] M. Sheikholeslami and D. Ganji, "Nanofluid hydrothermal behavior in existence of lorentz forces considering joule heating effect," *Journal of Molecular Liquids*, vol. 224, pp. 526–537, 2016.

[11] M. Sheikholeslami, D. Ganji, and M. Rashidi, "Magnetic field effect on unsteady nanofluid flow and heat transfer using buongiorno model," *Journal of Magnetism and Magnetic Materials*, vol. 416, pp. 164–173, 2016.

[12] N. Rudraswamy, B. Gireesha, and M. Krishnamurthy, "Effect of internal heat generation/absorption and viscous dissipation on mhd flow and heat transfer of nanofluid with particle suspension over a stretching surface," *Journal of Nanofluids*, vol. 5, no. 6, pp. 1000–1010, 2016.

[13] M. Sheikholeslami and A. J. Chamkha, "Influence of lorentz forces on nanofluid forced convection considering marangoni convection," *Journal of Molecular Liquids*, vol. 225, pp. 750–757, 2017.

[14] M. Sheikholeslami, M. Rashidi, and D. Ganji, "Effect of non-uniform magnetic field on forced convection heat transfer of fe3o4–water nanofluid," *Computer Methods in Applied Mechanics and Engineering*, vol. 294, pp. 299–312, 2015.

[15] M. Sheikholeslami, K. Vajravelu, and M. M. Rashidi, "Forced convection heat transfer in a semi annulus under the influence of a variable magnetic field," *International journal of heat and mass transfer*, vol. 92, pp. 339–348, 2016.

[16] M. Sheikholeslami, R.-u. Haq, A. Shafee, and Z. Li, "Heat transfer behavior of nanoparticle enhanced pcm solidification through an enclosure with v shaped

fins," *International Journal of Heat and Mass Transfer*, vol. 130, pp. 1322–1342, 2019.

[17] M. Sheikholeslami, "New computational approach for exergy and entropy analysis of nanofluid under the impact of lorentz force through a porous media," *Computer Methods in Applied Mechanics and Engineering*, vol. 344, pp. 319–333, 2019.

[18] M. Rashidi, M. Ali, N. Freidoonimehr, and F. Nazari, "Parametric analysis and optimization of entropy generation in unsteady mhd flow over a stretching rotating disk using artificial neural network and particle swarm optimization algorithm," *Energy*, vol. 55, pp. 497–510, 2013.

[19] M. Sheikholeslami, "Numerical approach for mhd al2o3-water nanofluid transportation inside a permeable medium using innovative computer method," *Computer Methods in Applied Mechanics and Engineering*, vol. 344, pp. 306–318, 2019.

[20] M. Rashidi, N. Kavyani, and S. Abelman, "Investigation of entropy generation in mhd and slip flow over a rotating porous disk with variable properties," *International Journal of Heat and Mass Transfer*, vol. 70, pp. 892–917, 2014.

[21] M. Sheikholeslami, "Influence of magnetic field on al2o3-h2o nanofluid forced convection heat transfer in a porous lid driven cavity with hot sphere obstacle by means of lbm," *Journal of Molecular Liquids*, vol. 263, pp. 472–488, 2018.

[22] M. Sheikholeslami, S. Shehzad, Z. Li, and A. Shafee, "Numerical modeling for alumina nanofluid magnetohydrodynamic convective heat transfer in a permeable medium using darcy law," *International Journal of Heat and Mass Transfer*, vol. 127, pp. 614–622, 2018.

[23] A. M. Siddiqui, S. Irum, and A. R. Ansari, "Unsteady squeezing flow of a viscous mhd fluid between parallel plates, a solution using the homotopy perturbation method," *Mathematical Modelling and Analysis*, vol. 13, no. 4, pp. 565–576, 2008.

[24] R. U. Haq, S. Nadeem, Z. Khan, and N. Noor, "Mhd squeezed flow of water functionalized metallic nanoparticles over a sensor surface," *Physica E: Low-dimensional Systems and Nanostructures*, vol. 73, pp. 45–53, 2015.

[25] H. Khan, M. Qayyum, O. Khan, and M. Ali, "Unsteady squeezing flow of casson fluid with magnetohydrodynamic effect and passing through porous medium," *Mathematical Problems in Engineering*, vol. 2016, 2016.

[26] A. Rashad, M. Rashidi, G. Lorenzini, S. E. Ahmed, and A. M. Aly, "Magnetic field and internal heat generation effects on the free convection in a rectangular cavity filled with a porous medium saturated with cu–water nanofluid," *International Journal of Heat and Mass Transfer*, vol. 104, pp. 878–889, 2017.

[27] N. Acharya, K. Das, and P. K. Kundu, "The squeezing flow of cu-water and cu-kerosene nanofluids between two parallel plates," *Alexandria Engineering Journal*, vol. 55, no. 2, pp. 1177–1186, 2016.

[28] S. A. Devi and S. S. U. Devi, "Numerical investigation of hydromagnetic hybrid cu–al2o3/water nanofluid flow over a permeable stretching sheet with suction," *International Journal of Nonlinear Sciences and Numerical Simulation*, vol. 17, no. 5, pp. 249–257, 2016.

[29] I. Waini, A. Ishak, and I. Pop, "Squeezed hybrid nanofluid flow over a permeable sensor surface," *Mathematics*, vol. 8, no. 6, p. 898, 2020.

[30] X. Su and Y. Yin, "Effects of an inclined magnetic field on the unsteady squeezing flow between parallel plates with suction/injection," *Journal of Magnetism and Magnetic Materials*, vol. 484, pp. 266–271, 2019.

[31] N. F. B. ISA, "Pat 152 fundamentals of fluid mechanics."

[32] Y. A. Cengel, *Fluid mechanics*. Tata McGraw-Hill Education, 2010.

[33] R. W. Fox, A. T. McDonald, and J. W. Mitchell, *Fox and McDonald's introduction to fluid mechanics*. John Wiley & Sons, 2020.

[34] W. M. Rohsenow, J. P. Hartnett, Y. I. Cho *et al.*, *Handbook of heat transfer*. McGraw-Hill New York, 1998, vol. 3.

[35] R. Bansal, *A textbook of fluid mechanics*. Firewall Media, 2005.

[36] J. H. Ferziger, M. Perić, and R. L. Street, *Computational methods for fluid dynamics*. Springer, 2002, vol. 3.

[37] T. Papanastasiou, G. Georgiou, and A. N. Alexandrou, *Viscous fluid flow*. CRC press, 2021.

[38] D. A. Anderson, J. C. Tannehill, R. H. Pletcher, M. Ramakanth, and V. Shankar, *Computational fluid mechanics and heat transfer*. CRC Press, 2020.

[39] J. N. Reddy and D. K. Gartling, *The finite element method in heat transfer and fluid dynamics*. CRC press, 2010.

[40] B. Lautrup, *Physics of continuous matter: exotic and everyday phenomena in the macroscopic world*. CRC press, 2011.

[41] J. Kunes, *Dimensionless physical quantities in science and engineering*. Elsevier, 2012.

[42] R. W. Lewis, P. Nithiarasu, and K. N. Seetharamu, *Fundamentals of the finite element method for heat and fluid flow*. John Wiley & Sons, 2004.

[43] X. Su and L. Zheng, "Hall effect on mhd flow and heat transfer of nanofluids over a stretching wedge in the presence of velocity slip and joule heating," *Central European Journal of Physics*, vol. 11, no. 12, pp. 1694–1703, 2013.

[44] N. A. L. Aladdin, N. Bachok, and I. Pop, "Cu-al2o3/water hybrid nanofluid flow over a permeable moving surface in presence of hydromagnetic and suction effects," *Alexandria Engineering Journal*, vol. 59, no. 2, pp. 657–666, 2020.